

Queueing Network Controls via Deep Reinforcement Learning

J. G. Dai^{1,2} and Mark Gluzman³

¹ School of Data Science, Shenzhen Research Institute of Big Data, The Chinese University of Hong Kong, Shenzhen

² School of Operations Research and Information Engineering, Cornell University, Ithaca, NY

³ Center for Applied Mathematics, Cornell University, Ithaca, NY

Abstract

Novel advanced policy gradient (APG) methods, such as Trust Region policy optimization and Proximal policy optimization (PPO), have become the dominant reinforcement learning algorithms because of their ease of implementation and good practical performance. A conventional setup for notoriously difficult queueing network control problems is a Markov decision problem (MDP) that has three features: infinite state space, unbounded costs, and long-run average cost objective. We extend the theoretical framework of these APG methods for such MDP problems. The resulting PPO algorithm is tested on a parallel-server system and large-size multiclass queueing networks. The algorithm consistently generates control policies that outperform state-of-art heuristics in literature in a variety of load conditions from light to heavy traffic. These policies are demonstrated to be near-optimal when the optimal policy can be computed.

A key to the successes of our PPO algorithm is the use of three variance reduction techniques in estimating the relative value function via sampling. First, we use a discounted relative value function as an approximation of the relative value function. Second, we propose regenerative simulation to estimate the discounted relative value function. Finally, we incorporate the approximating martingale-process method into the regenerative estimator.

Keywords: Multiclass Queueing Network, Control Variate, Reinforcement Learning, Long-Run Average Cost

1 Introduction

For more than 30 years, one of the most difficult problems in applied probability and operations research is to find a scalable algorithm for approximately solving the optimal control of stochastic processing networks, particularly when they are heavily loaded. These optimal control problems have many important applications including healthcare [25] and communications networks [79, 53], data centers [58, 55], and manufacturing systems [68, 48]. Stochastic processing networks are a broad class of models that were advanced in [32] and [33] and recently recapitulated and extended in [24].

In this paper, we demonstrate that a class of *deep reinforcement learning* algorithms known as proximal policy optimization (PPO), generalized from [73, 75] to our setting, can generate control policies that consistently beat the performance of all state-of-arts control policies known in the literature. The superior performances of our control policies appear to be robust as stochastic processing networks and their load conditions vary, with little or no problem-specific configurations of the algorithms.

Multiclass queueing networks (MQNs) are a special class of stochastic processing networks. They were introduced in [29] and have been studied intensively for more than 30 years for performance analysis and controls; see, for example, [34, 49, 12, 18, 87, 13, 14, 20, 38, 82]. Our paper focuses primarily on MQNs with long-run average cost objectives for two reasons. First, these stochastic control problems are notoriously difficult due to the size of the state space, particularly in heavy traffic. Second, a large body of research has motivated the development of various algorithms and control policies that are based on either heavy traffic asymptotic analysis or heuristics. See, for example, fluid policies [19], BIGSTEP policies [30], affine shift policies [59], discrete-review policies [54, 6], tracking policies [8], and “robust fluid” policies [14] in the former group and [52, 50] in the latter group. We demonstrate

that our algorithms outperform the state-of-art algorithms in [14]. In this paper, we will also consider an N -model that belongs to the family of parallel-server systems, another special class of stochastic processing networks. Unlike an MQN in which routing probabilities of jobs are fixed, a parallel-server system allows dynamic routing of jobs in order to achieve load-balancing among service stations. We demonstrate that our algorithms achieves near optimal performance in this setting, again with little special configuration of them.

For the queueing networks with Poisson arrival and exponential service time distribution, the control problems can be modeled within the framework of Markov decision processes (MDPs) [70] via uniformization. A typical algorithm for solving an MDP is via *policy iteration* or *value iteration*. However, in our setting, the corresponding MDP suffers from the usual curse of dimensionality: there are a large number of job classes, and the buffer capacity for each class is assumed to be infinite. Even with a truncation of the buffer capacity either as a mathematical convenience or a practical control technique, the resulting state space is huge when the network is large and heavily loaded.

A *reinforcement learning (RL) problem* often refers to a (*model-free*) MDP problem in which the underlying model governing the dynamics is not known, but sequences of data (actions, states, and rewards), known as episodes in this paper, can be observed under a given policy. It has been demonstrated that *RL algorithms* for solving RL problems can successfully overcome the curse of dimensionality in both the model-free and model-based MDP problems. Two factors are the keys to the success in a model-based MDP. First, Monte Carlo sampling method is used to approximately evaluate expectations. The sampling method also naturally supports the exploration needed in RL algorithms. Second, a parametric, low-dimensional representation of a value function and/or a policy can be used. In recent years, RL algorithms that use neural networks as an architecture for value function and policy parametrizations have shown state-of-art results [11, 62, 77, 66].

In recent years the Proximal Policy Optimization (PPO) algorithm [75] has become a default algorithm [72] for control optimization in new challenging environments including robotics [3], multiplayer video games [83, 66], neural network architecture engineering [89], molecular design [78]. In this paper we extend the PPO algorithm to MDP problems with *unbounded cost* functions and *long-run average cost* objectives. The original PPO algorithm [75] was proposed for problems with *bounded cost* function and *infinite-horizon discounted* objective. It was based on the trust region policy optimization (TRPO) algorithm developed in [73]. We use two separate feedforward neural networks, one for parametrization of the control policy and the other for value function approximation, a setup common to *actor-critic* algorithms [62]. We propose an approximating martingale-process (AMP) method for variance reduction to estimate policy value functions and show that the AMP estimation speeds up convergence of the PPO algorithm in the model-based setting. We provide a set of instructions for implementing the PPO algorithm specifically for MQNs. The instructions include the choice of initial stable randomized policy, methods for improving policy value function estimation, architecture of the value and policy neural networks, and the choice of hyperparameters. The proposed instructions can be potentially adapted to other advanced policy optimization RL algorithms, e.g. TRPO. Given the success of the PPO in various domains and its ease of use we focus on the PPO algorithm in this paper to illustrate efficiency of the deep RL framework for queueing control optimization.

The actor-critic methods can be considered as a combination of value-based and policy based methods. In a *value-based* approximate dynamic programming (ADP) algorithm, we may assume a low-dimensional approximation of the optimal value function (e.g. the optimal value function is a linear combination of known *features* [26, 71, 2]). Value-based ADP algorithm has dominated in the stochastic control of queueing networks literature; see, for example, [20, 63, 21, 82]. These algorithms however have not achieved robust empirical success for a wide class of control problems. It is now known that the optimal value function might have a complex structure which is hard to decompose on features, especially if decisions have effect over a long horizon [51].

In a *policy-based* ADP algorithm, we aim to learn the optimal policy directly. Policy gradient algorithms are used to optimize the objective value within a parameterized family of policies via gradient descent; see, for example, [56, 67, 69]. Although they are particularly effective for problems with high-dimensional action space, it might be difficult to reliably estimate the gradient of the value under the current policy. A direct sample-based estimation typically suffers from high variance in gradient estimation [69, Section 3], [56, Section 5], [9, Section 1.1.2]. Thus, actor-critic methods have been proposed [47] to estimate the value function and use it as a baseline and bootstrap for gradient direction approximation. The actor-critic method with Boltzmann parametrization of policies and linear approximation of the value functions has been applied for parallel-server system control in [16]. The standard policy

gradient methods typically perform one gradient update per data sample which yields poor data efficiency, and robustness, and an attempt to use a finite batch of samples to estimate the gradient and perform multiple steps of optimization “empirically ... leads to destructively large policy updates” [75]. In [75], the authors also note that the deep Q-learning algorithm [62] “fails on many simple problems”.

In [73, 75], the authors propose “*advanced policy gradient*” methods to overcome the aforementioned problems by designing novel objective functions that constrain the magnitude of policy updates to avoid performance collapse caused by large changes in the policy. In [73] the authors prove that minimizing a certain surrogate objective function guarantees decreasing the expected discounted cost. Unfortunately, their theoretically justified step-sizes of policy updates cannot be computed from available information for the RL algorithm. Trust Region Policy Optimization (TRPO) [73] has been proposed as a practical method to search for step-sizes of policy updates, and Proximal Policy Optimization (PPO) method [75] has been proposed to compute these step-sizes based on a clipped, “proximal” objective function.

We summarize the major contributions of our study:

1. In Section 3 we theoretically justify that the advanced policy gradient algorithms can be applied for long-run average cost MDP problems with countable state spaces and unbounded cost-to-go functions. We show that starting from a stable policy it is possible to improve long-run average performance with sufficiently small changes to the initial policy.
2. In Section 4.2 we discuss a new way to estimate relative value and advantage functions if transition probabilities are known. We adopt the approximating martingale-process method [36] which, to the best of our knowledge, has not been used in simulation-based approximate policy improvement setting.
3. In Section 4.3 we introduce a biased estimator of the relative value function through discounting the future costs. We interpret the discounting as the modification to the transition dynamics that shortens the regenerative cycles. We propose a regenerative estimator of the discounted relative value function.

The discounting combined with the AMP method and regenerative simulation significantly reduces the variance of the relative value function estimation at the cost of a tolerable bias. The use of the proposed variance reduction techniques speeds up the learning process of the PPO algorithm that we demonstrate by computational experiments in Section 5.1.

4. In Section 5 we conduct extensive computational experiments for multiclass queueing networks and parallel servers systems. We propose to choose architectures of neural networks automatically as the size of a queueing network varies. We demonstrate the effectiveness of these choices as well as other hyperparameter choices such as the learning rate used in gradient decent. We demonstrate that the performance of control policies resulting from the proposed PPO algorithm outperforms other heuristics.

2 Control of multiclass queueing networks

In this section we formulate the control problems for multiclass processing networks. We first give a formulation for the criss-cross network, which serves as an example, and then give a formulation for a general multiclass queueing network.

The set of real numbers is denoted by \mathbb{R} . The set of nonnegative integers is denoted by \mathbb{Z}_+ . For a vector a and a matrix A , a^T and A^T denote their transposes.

2.1 The criss-cross network

The criss-cross network has been studied in [35], [7], and [57] among others. The network depicted in Figure 1, which is taken from Figure 1.2 in [24], consists of two stations that process three classes of jobs. Each job class has its own dedicated buffer where jobs wait to be processed. All buffers are assumed to have an infinite capacity.

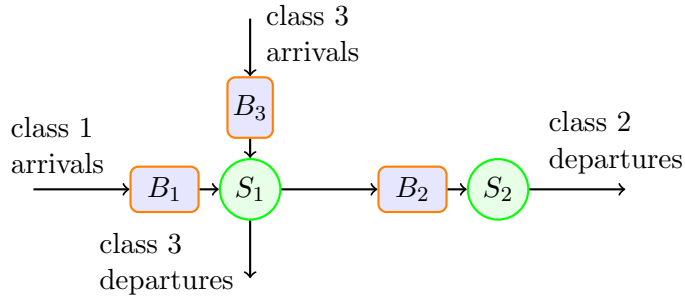


Figure 1: The criss-cross network

We assume that the jobs of class 1 and class 3 arrive to the system following Poisson processes with rates λ_1 and λ_3 , respectively. Server 1 processes both classes one job at a time. After being processed class 1 jobs become class 2 jobs and wait in buffer 2 for server 2 to process. Class 2 and class 3 jobs leave the system after their processings are completed. We assume that the processing times for class j jobs are i.i.d., having exponential distribution with mean m_j , $j = 1, 2, 3$. We denote $\mu_j := 1/m_j$ as the service rate of class j jobs. We assume that the following load conditions are satisfied:

$$\lambda_1 m_1 + \lambda_3 m_3 < 1 \quad \text{and} \quad \lambda_1 m_2 < 1. \quad (2.1)$$

Again, we assume each server processes one job at a time. Therefore, processor sharing among multiple jobs is not allowed for each server. Jobs within a buffer are processed in the first-in-first-out order. A service policy dictates the order in which jobs from different classes are processed. (See below for a precise definition of a stationary Markov policy.) We assume a decision time occurs when a new job arrives or a service is completed. For concreteness, we adopt a preemptive service policy — suppose the service policy dictates that server 1 processes a class 3 job next while it is in the middle of processing a class 1 job, the server preempts the unfinished class 1 job to start the processing of the leading class 3 job from buffer 3. Due to the memoryless property of an exponential distribution, it does not matter whether the preempted job keeps its remaining processing time or is assigned a new service time sampled from the original exponential distribution.

Under any service policy, at each decision time, the system manager needs to simultaneously choose action a_1 from set $\{0, 1, 3\}$ for server 1 and action a_2 from the set $\{0, 2\}$ for server 2; for server 1 to choose action j , $j = 1, 3$, means that server 1 processes a class j job next (if buffer j is non-empty), and to choose action 0 means that server 1 idles. Similarly, for server 2 to choose action 2 means that server 2 processes a class 2 job, and to choose action 0 means server 2 idles. Each server is allowed to choose action 0 even if there are waiting jobs at the associated buffers. Therefore, our service policies are not necessarily non-idling. We define the action set as $\mathcal{A} = \{(a_1, a_2) \in \{0, 1, 3\} \times \{0, 2\}\}$.

The service policy studied in this paper is *randomized*. By randomized, we mean each server takes a random action sampled from a certain distribution on the action set. For a set A , we use $\mathcal{P}(A)$ to denote the set of probability distributions on A . Therefore, for a pair $(p_1, p_2) \in \mathcal{P}(\{0, 1, 3\}) \times \mathcal{P}(\{0, 2\})$, server 1 takes a random action sampled from distribution p_1 and server 2 takes a random action sampled from distribution p_2 . For notational convenience, we note that a pair has a one-to-one correspondence to a vector u in the following set

$$\mathcal{U} = \{u = (u_1, u_2, u_3) \in \mathbb{R}_+^3 : u_1 + u_3 \leq 1 \text{ and } u_2 \leq 1\},$$

where $p_1 = (1 - u_1 - u_3, u_1, u_3) \in \mathcal{P}(\{0, 1, 3\})$ is a probability distribution on the action set $\{0, 1, 3\}$ and $p_2 = (1 - u_2, u_2) \in \mathcal{P}(\{0, 2\})$ is a probability distribution on the action set $\{0, 2\}$. Throughout this subsection, we use $u \in \mathcal{U}$ to denote pair (p_1, p_2) .

To define a randomized stationary Markovian service policy, let $x_j(t)$ be the number of class j jobs (including possibly one job in service) in the system at time t , $j = 1, 2, 3$. Then $x(t) = (x_1(t), x_2(t), x_3(t))$ is the vector of jobcounts at time t . Clearly, $x(t) \in \mathbb{Z}_+^3$. By convention, we assume the sample path of $\{x(t), t \geq 0\}$ is right continuous, which implies that when t is a decision time (triggered by an external arrival or a service completion), $x(t)$ has taken into account the arriving job or completed job at time t .

By a randomized stationary Markovian service policy we denote a map

$$\pi : \mathbb{Z}_+^3 \rightarrow \mathcal{U}.$$

Given this map π , at each decision time t , the system manager observes jobcounts $x = x(t)$, computes $\pi(x) \in \mathcal{U}$ and the corresponding pair $(p_1(x), p_2(x)) \in \mathcal{P}(\{0, 1, 3\}) \times \mathcal{P}(\{0, 2\})$. Then server 1 chooses a random action sampled from $p_1(x)$ and server 2 chooses a random action sampled from $p_2(x)$. When each distribution is concentrated on a single action, the corresponding policy is a *deterministic* stationary Markovian service policy. Hereafter, we use the term stationary Markovian service policies to mean randomized policies, which include deterministic service policies as special cases.

Under a stationary Markovian policy π , $\{x(t), t \geq 0\}$ is a continuous time Markov chain (CTMC). Hereafter, we call jobcount vector $x(t)$ the state at time t , and we denote the state space as $\mathcal{X} = \mathbb{Z}_+^3$. The objective of our optimal control problem is to find a stationary Markovian policy that minimizes the long-run average number of jobs in the network:

$$\inf_{\pi} \lim_{T \rightarrow \infty} \frac{1}{T} \mathbb{E}_{\pi} \int_0^T (x_1(t) + x_2(t) + x_3(t)) dt. \quad (2.2)$$

Because the interarrival and service times are exponentially distributed, the optimal control problem (2.2) fits the framework of semi-Markov decision process (SMDP). See, for example, [70, Chapter 11]. Indeed, one can easily verify that at each state x , taking action a , the distribution of the time interval until next decision time is exponential with rate $\beta(x, a)$ to be specified below. We use $P(y|x, a)$ to denote the transition probabilities of the embedded Markov decision process, where $y \in \mathcal{X}$ is a state at the next decision time. For any state $x \in \mathcal{X}$ and any action $a \in \mathcal{A}$, the following transition probabilities always hold

$$P((x_1 + 1, x_2, x_3)|x, a) = \frac{\lambda_1}{\beta(x, a)}, \quad P((x_1, x_2, x_3 + 1)|x, a) = \frac{\lambda_3}{\beta(x, a)}. \quad (2.3)$$

In the following, we specify $\beta(x, a)$ for each $(x, a) \in \mathcal{X} \times \mathcal{A}$ and additional transition probabilities. For action $a = (1, 2)$ and state $x = (x_1, x_2, x_2)$ with $x_1 \geq 1$ and $x_2 \geq 1$, $\beta(x, a) = \lambda_1 + \lambda_3 + \mu_1 + \mu_2$,

$$P((x_1 - 1, x_2 + 1, x_3)|x, a) = \frac{\mu_1}{\beta(x, a)}, \quad P((x_1, x_2 - 1, x_3)|x, a) = \frac{\mu_2}{\beta(x, a)};$$

for action $a = (3, 2)$ and state $x = (x_1, x_2, x_2)$ with $x_3 \geq 1$ and $x_2 \geq 1$, $\beta(x, a) = \lambda_1 + \lambda_3 + \mu_3 + \mu_2$,

$$P((x_1, x_2, x_3 - 1)|x, a) = \frac{\mu_3}{\beta(x, a)}, \quad P((x_1, x_2 - 1, x_3)|x, a) = \frac{\mu_2}{\beta(x, a)};$$

for action $a = (0, 2)$ and state $x = (x_1, x_2, x_3)$ with $x_2 \geq 1$, $\beta(x, a) = \lambda_1 + \lambda_3 + \mu_2$,

$$P((x_1, x_2 - 1, x_3)|x, a) = \frac{\mu_2}{\beta(x, a)};$$

for action $a = (1, 0)$ and state $x = (x_1, x_2, x_3)$ with $x_1 \geq 1$, $\beta(x, a) = \lambda_1 + \lambda_3 + \mu_1$,

$$P((x_1 - 1, x_2 + 1, x_3)|x, a) = \frac{\mu_1}{\beta(x, a)};$$

for action $a = (3, 0)$ and state $x = (x_1, x_2, x_3)$ with $x_3 \geq 1$, $\beta(x, a) = \lambda_1 + \lambda_3 + \mu_3$,

$$P((x_1, x_2, x_3 - 1)|x, a) = \frac{\mu_3}{\beta(x, a)};$$

for action $a = (0, 0)$ and state $x = (x_1, x_2, x_3)$, $\beta(x, a) = \lambda_1 + \lambda_3$. Also, $x_2 = 0$ implies that $a_2 = 0$, $x_1 = 0$ implies that $a_1 \neq 1$, and $x_3 = 0$ implies that $a_1 \neq 3$.

Because the time between state transitions are exponentially distributed, we adopt the method of uniformization for solving the SMDP; see, for example, [76] and [70, Chapter 11]. We denote

$$B = \lambda_1 + \lambda_3 + \mu_1 + \mu_2 + \mu_3. \quad (2.4)$$

For the new control problem under uniformization, the decision times are determined by the arrival times of a Poisson process with (uniform) rate B that is independent of the underlying state. Given current state $x \in \mathcal{X}$ and action $a \in \mathcal{A}$, new transition probabilities into $y \in \mathcal{X}$ are given by

$$\tilde{P}(y|x, a) = \begin{cases} P(y|x, a)\beta(x, a)/B & \text{if } x \neq y, \\ 1 - \beta(x, a)/B & \text{otherwise.} \end{cases} \quad (2.5)$$

The transition probabilities \tilde{P} in (2.5) will define a (discrete time) MDP. The objective is given by

$$\inf_{\pi} \lim_{N \rightarrow \infty} \frac{1}{N} \mathbb{E}_{\pi} \left[\sum_{k=0}^{N-1} \left(x_1^{(k)} + x_2^{(k)} + x_3^{(k)} \right) \right], \quad (2.6)$$

where π belongs to the family of stationary Markov policies, and $x^{(k)} = \left(x_1^{(k)}, x_2^{(k)}, x_3^{(k)} \right)$ is the state (vector of jobcounts) at the time of the k th decision (in the uniformized framework). Under a stationary Markov policy π , $\{x^{(k)} : k = 0, 1, 2, \dots\}$ is a discrete time Markov chain (DTMC).

The existence of a stationary Markovian policy π^* that minimizes (2.6) follows from [59, Theorem 4.3] if the load conditions (2.1) are satisfied. Under a mild condition on π^* , which can be shown to be satisfied following the argument in [59, Theorem 4.3], the policy π^* is an optimal Markovian stationary policy for (2.2) [15, Theorem 2.1]. Moreover, under policy π^* , the objective in (2.2) is equal to that in (2.6); see [15, Theorem 3.6].

2.2 General formulation of a multiclass queueing network control problem

We consider a multiclass queueing network that has L stations and J job classes. For notational convenience we denote $\mathcal{L} = \{1, \dots, L\}$ as the set of stations, $\mathcal{J} = \{1, \dots, J\}$ as the set of job classes. Each station has a single server that processes jobs from the job classes that belong to the station. Each job class belongs to one station. We use $\ell = s(j) \in \mathcal{L}$ to denote the station that class j belongs to. We assume the function $s : \mathcal{J} \rightarrow \mathcal{L}$ satisfies $s(\mathcal{J}) = \mathcal{L}$. Jobs arrive externally and are processed sequentially at various stations, moving from one class to the next after each processing step until they exit the network. Upon arrival if a class j job finds the associated server busy, the job waits in the corresponding buffer j . We assume that every buffer has an infinite capacity. For each station $\ell \in \mathcal{L}$, we define

$$\mathcal{B}(\ell) := \{j \in \mathcal{J} : s(j) = \ell\} \quad (2.7)$$

as the set of job classes to be processed by server ℓ .

Class $j \in \mathcal{J}$ jobs arrive externally to buffer j following a Poisson process with rate λ_j ; when $\lambda_j = 0$, there are no external arrivals into buffer j . Class j jobs are processed by server $s(j)$ following the service policy as specified below. We assume the service times for class j jobs are i.i.d. having exponential distribution with mean $1/\mu_j$. Class j job, after being processed by server $s(j)$, becomes class $k \in \mathcal{J}$ job with probability r_{jk} and leaves the network with probability $1 - \sum_{k=1}^K r_{jk}$. We define $J \times J$ matrix $R := (r_{jk})_{j,k=1,\dots,J}$ as the routing matrix. We assume that the network is open, meaning that $I - R$ is invertible. We let vector $q = (q_1, q_2, \dots, q_J)^T$ satisfy the system of linear equations

$$q = \lambda + R^T q. \quad (2.8)$$

Equation (2.8) is known as the traffic equation, and it has a unique solution under the open network assumption. For each class $j \in \mathcal{J}$, q_j is interpreted to be the total arrival rate into buffer j , considering both the external arrivals and internal arrivals from service completions at stations. We define the load ρ_{ℓ} of station $\ell \in \mathcal{L}$ as

$$\rho_{\ell} := \sum_{j \in \mathcal{B}(\ell)} \frac{q_j}{\mu_j}.$$

We assume that

$$\rho_{\ell} < 1 \quad \text{for each station } \ell \in \mathcal{L}. \quad (2.9)$$

We let $x(t) = (x_1(t), \dots, x_J(t))$ be the vector of jobcounts at time t . A decision time occurs when a new job arrives at the system or a service is completed. Under any service policy, at each decision time, the system manager needs to simultaneously choose an action for each server $\ell \in \mathcal{L}$. For each server $\ell \in \mathcal{L}$ the system manager selects an action from set $\mathcal{B}(\ell) \cup \{0\}$: action $j \in \mathcal{B}(\ell)$ means that the system manager gives priority to job class j at station ℓ ; action 0 means server ℓ idles until the next decision time.

We define set

$$\mathcal{U} = \left\{ u = (u_1, u_2, \dots, u_J) \in \mathbb{R}_+^J : \sum_{j \in \mathcal{B}(\ell)} u_j \leq 1 \text{ for each } \ell \in \mathcal{L} \right\}. \quad (2.10)$$

For each station $\ell \in \mathcal{L}$ vector $u \in \mathcal{U}$ defines a probability distribution u_ℓ on the action set $\mathcal{B}(\ell) \cup \{0\}$: probability of action j is equal to u_j for $j \in \mathcal{B}(\ell)$, and probability of action 0 is equal to $\left(1 - \sum_{j \in \mathcal{B}(\ell)} u_j\right)$.

We define a randomized stationary Markovian service policy as a map from a set of jobcount vectors into set \mathcal{U} defined in (2.10):

$$\pi : \mathbb{Z}_+^J \rightarrow \mathcal{U}.$$

Given this map π , at each decision time t , the system manager observes jobcounts $x(t)$, chooses $\pi(x) \in \mathcal{U}$, and based on $\pi(x)$ computes probability distribution u_ℓ for each $\ell \in \mathcal{L}$. Then the system manager independently samples one action from u_ℓ for each server $\ell \in \mathcal{L}$.

The objective is to find a stationary Markovian policy π that minimizes the long-run average number of jobs in the network:

$$\inf_{\pi} \lim_{T \rightarrow \infty} \frac{1}{T} \mathbb{E}_{\pi} \int_0^T \left(\sum_{j=1}^J x_j(t) \right) dt. \quad (2.11)$$

Under a stationary Markovian policy π , we adopt the method of uniformization to obtain a uniformized discrete time Markov chain (DTMC) $\{x^{(k)} : k = 0, 1, \dots\}$. We abuse the notation and denote a system state as $x^{(k)} = \left(x_1^{(k)}, x_2^{(k)}, \dots, x_J^{(k)}\right)$ after k transitions of the DTMC.

In this paper, we develop algorithms to approximately solve the following (discrete-time) MDP problem:

$$\inf_{\pi} \lim_{N \rightarrow \infty} \frac{1}{N} \mathbb{E}_{\pi} \left[\sum_{k=0}^{N-1} \sum_{j=1}^J x_j^{(k)} \right]. \quad (2.12)$$

Remark 1. It has been proved in [59] that the MDP (2.12) has an optimal policy that satisfies the conditions in [15, Theorem 3.6] if the “fluid limit model” under some policy is L_2 -stable. Under the load condition (2.9), conditions in [59] can be verified as follows. First, we adopt the randomized version of the head-of-line static processor sharing (HLSPS) as defined in [24, Section 4.6]. We apply this randomized policy to the discrete-time MDP to obtain the resulting DTMC. The fluid limit path of this DTMC can be shown to satisfy the fluid model defined in [24, Definition 8.17] following a procedure that is similar to, but much simpler than, the proof of [24, Theorem 12.24]. Finally, [24, Theorem 8.18] shows the fluid model is stable, which is stronger than the L_2 -stability needed.

3 Reinforcement learning approach for queueing network control

Originally, policy gradient algorithms have been developed to find optimal policies which optimize the finite horizon total cost or infinite horizon discounted total cost objectives. For stochastic processing networks and their applications, it is often useful to optimize the long-run average cost. In this section we develop a version of the Proximal Policy Optimization algorithm. See Section 5, which demonstrates the effectiveness of our proposed PPO for finding the near optimal control policies for stochastic processing networks.

3.1 Positive recurrence and \mathcal{V} -uniform ergodicity

As discussed in Section 2, operating under a fixed randomized stationary control policy, the dynamics of a stochastic processing network is a DTMC. We restrict policies so that the resulting DTMCs are irreducible and aperiodic. Such a DTMC does not always have a stationary distribution. When the

DTMC does not have a stationary distribution, the performance of the control policy is necessarily poor, leading to an infinite long-run average cost. It is well known that an irreducible DTMC has a unique stationary distribution if and only if it is positive recurrent. Hereafter, when the DTMC is positive recurrent, we call the corresponding control policy *stable*. Otherwise, we call it *unstable*.

A sufficient condition for an irreducible DTMC to be positive recurrent is the Foster-Lyapunov drift condition. The drift condition (3.1) in the following lemma is stronger than the classical Foster-Lyapunov drift condition. For a proof of the lemma, see Theorem 11.3.4 and Theorem 14.3.7 in [61].

Lemma 1. *Consider an irreducible Markov chain on a countable state space \mathcal{X} with a transition matrix P on $\mathcal{X} \times \mathcal{X}$. Assume there exists a vector $\mathcal{V} : \mathcal{X} \rightarrow [1, \infty)$ such that the following drift condition holds for some constants $b \in (0, 1)$ and $d \geq 0$, and a finite subset $C \subset \mathcal{X}$:*

$$\sum_{y \in \mathcal{X}} P(y|x)\mathcal{V}(y) \leq b\mathcal{V}(x) + d\mathbb{I}_C(x), \quad \text{for each } x \in \mathcal{X}, \quad (3.1)$$

where $\mathbb{I}_C(x) = 1$ if $x \in C$ and $\mathbb{I}_C(x) = 0$ otherwise. Here, $P(y|x) = P(x, y)$ is the transition probability from state $x \in \mathcal{X}$ to state $y \in \mathcal{X}$. Then (a) the Markov chain with the transition matrix P is positive recurrent with a unique stationary distribution μ ; and (b) $\mu^T \mathcal{V} < \infty$, where for any function $f : \mathcal{X} \rightarrow \mathbb{R}$ we define $\mu^T f$ as

$$\mu^T f := \sum_{x \in \mathcal{X}} \mu(x)f(x).$$

Vector \mathcal{V} in the drift condition (3.1) is called a *Lyapunov function* for the Markov chain. For any matrix M on $\mathcal{X} \times \mathcal{X}$, its \mathcal{V} -norm is defined to be

$$\|M\|_{\mathcal{V}} = \sup_{x \in \mathcal{X}} \frac{1}{\mathcal{V}(x)} \sum_{y \in \mathcal{X}} |M(x, y)|\mathcal{V}(y).$$

An irreducible, aperiodic Markov chain with transition matrix P is called \mathcal{V} -uniformly ergodic if

$$\|P^n - \Pi\|_{\mathcal{V}} \rightarrow 0 \text{ as } n \rightarrow \infty,$$

where every row of Π is equal to the stationary distribution μ , i.e. $\Pi(x, y) := \mu(y)$, for any $x, y \in \mathcal{X}$. The drift condition (3.1) is sufficient and necessary for an irreducible, aperiodic Markov chain to be \mathcal{V} -uniformly ergodic [61, Theorem 16.0.1]. For an irreducible, aperiodic Markov chain that satisfies (3.1), for any $g : \mathcal{X} \rightarrow \mathbb{R}$ with $|g(x)| \leq \mathcal{V}(x)$ for $x \in \mathcal{X}$, there exist constants $R < \infty$ and $r < 1$ such that

$$\left| \sum_{y \in \mathcal{X}} P^n(y|x)g(y) - \mu^T g \right| \leq R\mathcal{V}(x)r^n \quad (3.2)$$

for any $x \in \mathcal{X}$ and $n \geq 0$; see [61, Theorem 15.4.1].

3.2 Poisson equation

For an irreducible DTMC on state space \mathcal{X} (possibly infinite) with transition matrix P , we assume that there exists a Lyapunov function \mathcal{V} satisfying (3.1). For any cost function $g : \mathcal{X} \rightarrow \mathbb{R}$ satisfying $|g(x)| \leq \mathcal{V}(x)$ for each $x \in \mathcal{X}$, it follows from Lemma 1 that $\mu^T |g| < \infty$. Lemma 2 below asserts that the following equation has a solution $h : \mathcal{X} \rightarrow \mathbb{R}$:

$$g(x) - \mu^T g + \sum_{y \in \mathcal{X}} P(y|x)h(y) - h(x) = 0 \quad \text{for each } x \in \mathcal{X}. \quad (3.3)$$

Equation (3.3) is called a *Poisson equation* of the Markov chain with transition matrix P and cost function g . Function $h : \mathcal{X} \rightarrow \mathbb{R}$ that satisfies (3.3) is called a *solution* to the Poisson equation. The solution is unique up to a constant shift, namely, if h_1 and h_2 are two solutions to Poisson equation (3.3) with $\mu^T(|h_1| + |h_2|) < \infty$, then there exists a constant $b \in \mathbb{R}$ such that $h_1(x) = h_2(x) + b$ for each $x \in \mathcal{X}$, see [61, Proposition 17.4.1].

A solution h to the Poisson equation is called a *fundamental solution* if $\mu^T h = 0$. The proof of the following lemma is provided in [60, Proposition A.3.11].

Lemma 2. Consider a \mathcal{V} -uniformly ergodic Markov chain with transition matrix P and the stationary distribution μ . For any cost function $g : \mathcal{X} \rightarrow \mathbb{R}$ satisfying $|g| \leq \mathcal{V}$, Poisson equation (3.3) admits a fundamental solution

$$h^{(f)}(x) := \mathbb{E} \left[\sum_{k=0}^{\infty} \left(g(x^{(k)}) - \mu^T g \right) \mid x^{(0)} = x \right] \text{ for each } x \in \mathcal{X}, \quad (3.4)$$

where $x^{(k)}$ is the state of the Markov chain after k timesteps.

We define fundamental matrix Z of the Markov chain with transition kernel P as

$$Z := \sum_{k=0}^{\infty} (P - \Pi)^k. \quad (3.5)$$

It follows from [61, Theorem 16.1.2] that the series (3.5) converges in \mathcal{V} -norm and, moreover, $\|Z\|_{\mathcal{V}} < \infty$. Then, it is easy to see that fundamental matrix Z is an inverse matrix of $(I - P + \Pi)$, i.e. $Z(I - P + \Pi) = (I - P + \Pi)Z = I$. See Appendix Section A for the proof of the following Lemma 3.

Lemma 3. Fundamental matrix Z maps any cost function $|g| \leq \mathcal{V}$ into a corresponding fundamental solution $h^{(f)}$ defined by (3.4):

$$h^{(f)} = Z (g - (\mu^T g)e), \quad (3.6)$$

where $e = (1, 1, \dots, 1, \dots)^T$ is a unit vector.

Remark 2. Consider matrices A, B, C on $\mathcal{X} \times \mathcal{X}$. The associativity property,

$$ABC = (AB)C = A(BC),$$

does not always hold for matrices defined on a countable state space; see a counterexample in [45, Section 1.1]. However, if $\|A\|_{\mathcal{V}} < \infty, \|B\|_{\mathcal{V}} < \infty, \|C\|_{\mathcal{V}} < \infty$ then matrices A, B, C associate, see [42, Lemma 2.1]. Hence, there is no ambiguity in the definition of the fundamental matrix (3.5):

$$(P - \Pi)^k = (P - \Pi)(P - \Pi)^{k-1} = (P - \Pi)^{k-1}(P - \Pi), \text{ for } k \geq 1$$

where $\|P - \Pi\|_{\mathcal{V}} < \infty$ holds due to the drift condition (3.1).

3.3 Improvement guarantee for average cost objective

We consider an MDP problem with a countable state space \mathcal{X} , finite action space \mathcal{A} , one-step cost function $g(x)$, and transition function $P(\cdot|x, a)$. For each state-action pair (x, a) , we assume that the chain can transit to a finite number of distinguished states, i.e. set $\{y \in \mathcal{X} : P(y|x, a) > 0\}$ is finite for each $(x, a) \in \mathcal{X} \times \mathcal{A}$.

We consider $\Theta \subset \mathbb{R}^d$ for some integer $d > 0$ and Θ is open. With every $\theta \in \Theta$, we associate a randomized Markovian policy π_{θ} , which at any state $x \in \mathcal{X}$ chooses action $a \in \mathcal{A}$ with probability $\pi_{\theta}(a|x)$. Under policy π_{θ} , the corresponding DTMC has transition matrix P_{θ} given by

$$P_{\theta}(x, y) = \sum_{a \in \mathcal{A}} \pi_{\theta}(a|x) P(y|x, a) \text{ for } x, y \in \mathcal{X}.$$

For each $\theta \in \Theta$ we assume that the resulting Markov chain with transition probabilities P_{θ} is irreducible and aperiodic.

We also assume there exists $\eta \in \Theta$ such that the drift condition (3.1) is satisfied for the transition matrix P_{η} with a Lyapunov function $\mathcal{V} : \mathcal{X} \rightarrow [1, \infty)$. By Lemma 2 the corresponding fundamental matrix Z_{η} is well-defined. The following lemma says that if P_{η} is positive recurrent and P_{θ} is ‘‘close’’ to P_{η} , then P_{θ} is also positive recurrent. See Appendix Section A for the proof.

Lemma 4. Fix an $\eta \in \Theta$. We assume that drift condition (3.1) holds for P_{η} . Let some $\theta \in \Theta$ satisfies,

$$\|(P_{\theta} - P_{\eta})Z_{\eta}\|_{\mathcal{V}} < 1,$$

then the Markov chain with transition matrix P_{θ} has a unique stationary distribution μ_{θ} .

Assume the assumption of Lemma 4 holds. For any cost function $|g| \leq \mathcal{V}$, we denote the corresponding fundamental solution to the Poisson equation as h_η and the long-run average cost

$$\mu_\eta^T g := \sum_{x \in \mathcal{X}} \mu_\eta(x) g(x). \quad (3.7)$$

The following theorem provides a bound on the difference of long-run average performance of policies π_θ and π_η . See Appendix Section A for the proof.

Theorem 1. *Suppose that the Markov chain with transition matrix P_η is an irreducible chain such that the drift condition (3.1) holds for some function $\mathcal{V} \geq 1$ and the cost function satisfies $|g| < \mathcal{V}$.*

For any $\theta \in \Theta$ such that

$$D_{\theta, \eta} := \|(P_\theta - P_\eta)Z_\eta\|_{\mathcal{V}} < 1 \quad (3.8)$$

the difference of long-run average costs of policies π_θ and π_η is bounded by:

$$\mu_\theta^T g - \mu_\eta^T g \leq N_1(\theta, \eta) + N_2(\theta, \eta), \quad (3.9)$$

where $N_1(\theta, \eta)$, $N_2(\theta, \eta)$ are finite and equal to

$$N_1(\theta, \eta) := \mu_\eta^T (g - (\mu_\eta^T g)e + P_\theta h_\eta - h_\eta), \quad (3.10)$$

$$N_2(\theta, \eta) := \frac{D_{\theta, \eta}^2}{1 - D_{\theta, \eta}} \|g - (\mu_\eta^T g)e\|_{\infty, \mathcal{V}} (\mu_\eta^T \mathcal{V}), \quad (3.11)$$

where, for a vector ν on \mathcal{X} , \mathcal{V} -norm is defined as

$$\|\nu\|_{\infty, \mathcal{V}} := \sup_{x \in \mathcal{X}} \frac{|\nu(x)|}{\mathcal{V}(x)}. \quad (3.12)$$

It follows from Theorem 1 that the negativity of the right side of inequality (3.9) guarantees that policy π_θ yields an improved performance compared with the initial policy π_η . Since

$$\min_{\theta \in \Theta: D_{\theta, \eta} < 1} [N_1(\theta, \eta) + N_2(\theta, \eta)] \leq N_1(\eta, \eta) + N_2(\eta, \eta) = 0,$$

we want to find $\theta = \theta^*$:

$$\theta^* = \operatorname{argmin}_{\theta \in \Theta: D_{\theta, \eta} < 1} [N_1(\theta, \eta) + N_2(\theta, \eta)] \quad (3.13)$$

to achieve the maximum improvement in the upper bound (3.9). In the setting of finite horizon and infinite discounted RL problems, [44, 73] propose to fix the maximum change between policies π_θ and π_η by bounding the $N_2(\theta, \eta)$ term and to minimize $N_1(\theta, \eta)$. Below, we discuss the motivation for developing the PPO algorithm proposed in Section 3.4, leading to a practical algorithm to approximately solve optimization (3.13).

First, we observe that

$$\begin{aligned} |N_1(\theta, \eta)| &:= |\mu_\eta^T (g - (\mu_\eta^T g)e + P_\theta h_\eta - h_\eta)| \\ &\leq (\mu_\eta^T \mathcal{V}) \|g - (\mu_\eta^T g)e + P_\theta h_\eta - h_\eta\|_{\infty, \mathcal{V}} \\ &= (\mu_\eta^T \mathcal{V}) \|(P_\theta - P_\eta)h_\eta\|_{\infty, \mathcal{V}} \\ &= (\mu_\eta^T \mathcal{V}) \|(P_\theta - P_\eta)Z_\eta (g - (\mu_\eta^T g)e)\|_{\infty, \mathcal{V}} \\ &\leq (\mu_\eta^T \mathcal{V}) \|g - (\mu_\eta^T g)e\|_{\infty, \mathcal{V}} D_{\theta, \eta}. \end{aligned}$$

Therefore, when θ is close to η , we expect that $D_{\theta, \eta}$ in (3.8) is small and $N_1(\theta, \eta) = O(D_{\theta, \eta})$.

From (3.11), $N_2(\theta, \eta)$ is nonnegative and $N_2(\theta, \eta) = O(D_{\theta, \eta}^2)$. Therefore, when $N_1(\theta, \eta) < 0$ and $D_{\theta, \eta}$ is small enough, π_θ is a strict improvement over π_η . Lemma 5 shows that the distance $D_{\theta, \eta}$ can be controlled by the probability ratio

$$r_{\theta, \eta}(a|x) := \frac{\pi_\theta(a|x)}{\pi_\eta(a|x)} \quad (3.14)$$

between the two policies.

Lemma 5. *Suppose that the Markov chain with transition matrix P_η is an irreducible chain such that the drift condition (3.1) holds for some function $\mathcal{V} \geq 1$ and the cost function satisfies $|g| < \mathcal{V}$. Then for any $\theta \in \Theta$*

$$D_{\theta,\eta} \leq \|Z_\eta\|_{\mathcal{V}} \sup_{x \in \mathcal{X}} \sum_{a \in \mathcal{A}} |r_{\theta,\eta}(a|x) - 1| G_\eta(x, a),$$

$$\text{where } G_\eta(x, a) := \frac{1}{\mathcal{V}(x)} \sum_{y \in \mathcal{X}} \pi_\eta(a|x) P(y|x, a) \mathcal{V}(y).$$

Lemma 5 implies that $D_{\theta,\eta}$ is small when the ration $r_{\theta,\eta}(a|x)$ in (3.14) is close to 1 for each state-action pair (x, a) . Note that $r_{\theta,\eta}(a|x) = 1$ and $D_{\theta,\eta} = 0$ when $\theta = \eta$. See Appendix Section A for the proof.

3.4 Proximal Policy Optimization

We rewrite the first term of the right-hand side of (3.9) as:

$$\begin{aligned} N_1(\theta, \eta) &= \mu_\eta^T (g - (\mu_\eta^T g)e + P_\theta h_\eta - h_\eta) \\ &= \mathbb{E}_{\substack{x \sim \mu_\eta \\ a \sim \pi_\theta(\cdot|x) \\ y \sim P(\cdot|x, a)}} [g(x) - (\mu_\eta^T g)e + h_\eta(y) - h_\eta(x)] \\ &= \mathbb{E}_{\substack{x \sim \mu_\eta \\ a \sim \pi_\theta(\cdot|x)}} A_\eta(x, a) \\ &= \mathbb{E}_{\substack{x \sim \mu_\eta \\ a \sim \pi_\eta(\cdot|x)}} \left[\frac{\pi_\theta(a|x)}{\pi_\eta(a|x)} A_\eta(x, a) \right] = \mathbb{E}_{\substack{x \sim \mu_\eta \\ a \sim \pi_\eta(\cdot|x)}} [r_{\theta,\eta}(a|x) A_\eta(x, a)], \end{aligned} \quad (3.15)$$

where we define an advantage function $A_\eta : \mathcal{X} \times \mathcal{A} \rightarrow \mathbb{R}$ of policy π_η , $\eta \in \Theta$ as:

$$A_\eta(x, a) := \mathbb{E}_{y \sim P(\cdot|x, a)} [g(x) - \mu_\eta^T g + h_\eta(y) - h_\eta(x)]. \quad (3.16)$$

Equation (3.15) implies that if we want to minimize $N_1(\theta, \eta)$, then the ratio $r_{\theta,\eta}(a|x)$ should be minimized (w.r.t. θ) when $A_\eta(x, a) > 0$, and maximized when $A_\eta(x, a) < 0$ for each $x \in \mathcal{X}$. The end of Section 3.3 suggests that we should strive to (a)

$$\text{minimize } N_1(\theta, \eta), \quad (3.17)$$

and (b) keep the ratio $r_{\theta,\eta}(a|x)$ in (3.14) close to 1. In [75] the authors propose to minimize (w.r.t. $\theta \in \Theta$) the following clipped surrogate objective

$$L(\theta, \eta) := \mathbb{E}_{\substack{x \sim \mu_\eta \\ a \sim \pi_\eta(\cdot|x)}} \max [r_{\theta,\eta}(a|x) A_\eta(x, a), \text{clip}(r_{\theta,\eta}(a|x), 1 - \epsilon, 1 + \epsilon) A_\eta(x, a)], \quad (3.18)$$

where $\epsilon \in (0, 1)$ is a hyperparameter, and clipping function is defined as

$$\text{clip}(c, 1 - \epsilon, 1 + \epsilon) := \begin{cases} \max(1 - \epsilon, c), & \text{if } c \leq 1, \\ \min(1 + \epsilon, c), & \text{otherwise.} \end{cases}$$

In [75] the authors coined the term, proximal policy optimization (PPO), for their algorithm, and demonstrated its ease of implementation and its ability to find good control policies.

The objective term $\text{clip}(r_{\theta,\eta}(a|x), 1 - \epsilon, 1 + \epsilon) A_\eta(x, a)$ in (3.18) prevents changes to the policy that move $r_{\theta,\eta}(a|x)$ far from 1. Then the objective function (3.18) is an upper bound (i.e. a pessimistic bound) on the unclipped objective (3.17). Thus, an improvement on the objective (3.18) translates to an improvement on $N_1(\theta, \eta)$ only when $\theta \in \Theta$ satisfies $r_{\theta,\eta} \in (1 - \epsilon, 1 + \epsilon)$. The alternative heuristics proposed in [73, 86, 75, 88] to solve optimization problem (3.13): each defines a loss function that controls $N_2(\theta, \eta)$ and minimizes the $N_1(\theta, \eta)$ term. Following [75], we use loss function (3.18) because of its implementation simplicity.

To compute objective function in (3.18) we first evaluate the expectation and precompute advantage functions in (3.18). We assume that an approximation $\hat{A}_\eta : \mathcal{X} \times \mathcal{A} \rightarrow \mathbb{R}$ of the advantage function (3.16)

is available and focus on estimating the objective from simulations. See Section 4 below for estimating \hat{A}_η .

Given an episode with length N generated under policy π_η we compute the advantage function estimates $\hat{A}_\eta(x^{(k,q)}, a^{(k,q)})$ at the observed state-action pairs:

$$D^{(0:N-1)} := \left\{ \left(x^{(0)}, a^{(0)}, \hat{A}_\eta(x^{(0)}, a^{(0)}) \right), \left(x^{(1)}, a^{(1)}, \hat{A}_\eta(x^{(1)}, a^{(1)}) \right), \dots, \left(x^{(N-1)}, a^{(N-1)}, \hat{A}_\eta(x^{(N-1)}, a^{(N-1)}) \right) \right\},$$

and estimate the loss function (3.18) as a sample average over the state-action pairs from the episode:

$$\hat{L}(\theta, \eta, D^{(0:N-1)}) = \sum_{k=0}^{N-1} \max \left[\frac{\pi_\theta(a^{(k)}|x^{(k)})}{\pi_\eta(a^{(k)}|x^{(k)})} \hat{A}_\eta(x^{(k)}, a^{(k)}), \text{clip} \left(\frac{\pi_\theta(a^{(k)}|x^{(k)})}{\pi_\eta(a^{(k)}|x^{(k)})}, 1 - \epsilon, 1 + \epsilon \right) \hat{A}_\eta(x^{(k)}, a^{(k)}) \right]. \quad (3.19)$$

In theory, one long episode under policy π_η starting from any initial state $x^{(0)}$ is sufficient because the following SLLN for Markov chains holds: with probability 1,

$$\lim_{N \rightarrow \infty} \frac{1}{N} \hat{L}(\theta, \eta, D^{(0:N-1)}) = L(\theta, \eta).$$

4 Advantage function estimation

The computation of objective function (3.18) relies on the availability of an estimate of advantage function $A_\eta(x, a)$ in (3.16). We assume our MDP model is known. So the expectation on (3.16) can be computed exactly, and we can perform the computation in a timely manner. In this section, we explain how to estimate h_η , a solution to the Poisson equation (3.3) with $P = P_\eta$ and $\mu = \mu_\eta$.

To compute expectation $A(x^{(k)}, a^{(k)})$ in (3.16) for a given state-action pair $(x^{(k)}, a^{(k)})$, we need to evaluate $h_\eta(y)$ for each y that is reachable from $x^{(k)}$. This requires one to estimate $h_\eta(y)$ for some states y that have not been visited in the simulation. Our strategy is to use Monte Carlo method to estimate $h_\eta(y)$ at a selected subset of y 's, and then use an approximator $f_\psi(y)$ to replace $h_\eta(y)$ for an arbitrary $y \in \mathcal{X}$. The latter is standard in deep learning. Therefore, we focus on finding a good estimator $\hat{h}(y)$ for $h_\eta(y)$.

4.1 Regenerative estimation

Lemma 2 provides a representation of the fundamental solution (3.4) for h_η . Unfortunately, the known unbiased Monte Carlo estimators of the fundamental solution rely on obtaining samples from the stationary distribution of the Markov chain [22, Section 5.1].

We define the following solution to the Poisson equation (3.3).

Lemma 6. *Consider the \mathcal{V} -uniformly ergodic Markov chain with transition matrix P and the stationary distribution μ . Let $x^* \in X$ be an arbitrary state of the positive recurrent Markov chain. For any cost function $g : \mathcal{X} \rightarrow \mathbb{R}$ such that $|g| \leq \mathcal{V}$, the Poisson's equation (3.3) admits a solution*

$$h^{(x^*)}(x) := \mathbb{E} \left[\sum_{k=0}^{\sigma(x^*)-1} \left(g(x^{(k)}) - \mu^T g \right) \mid x^{(0)} = x \right] \text{ for each } x \in \mathcal{X}, \quad (4.1)$$

where $\sigma(x^*) = \min \{k > 0 \mid x^{(k)} = x^*\}$ is the first future time when state x^* is visited. Furthermore, the solution has a finite \mathcal{V} -norm: $\|h^{(x^*)}\|_{\infty, \mathcal{V}} < \infty$.

See [60, Proposition A.3.1] for the proof. Here, we refer to state x^* as a *regeneration state*, and to the times $\sigma(x^*)$ when the regeneration state is visited as *regeneration times*.

The value of advantage function (3.16) does not depend on a particular choice of a solution of the Poisson equation (3.3) since if h_1 and h_2 are two solutions such that $\mu^T(|h_1| + |h_2|) < \infty$, then there exists a constant $b \in \mathbb{R}$ such that $h_1(x) = h_2(x) + b$ for each $x \in \mathcal{X}$, [61, Proposition 17.4.1]. Therefore, we use representation (4.1) for h_η in computing (3.16).

We assume that an episode consisting of N regenerative cycles

$$\left\{ x^{(0)}, x^{(1)}, \dots, x^{(\sigma_1)}, \dots, x^{(\sigma_N-1)} \right\}$$

has been generated under policy π_η , where $x^{(0)} = x^*$.

We compute an estimate of the long-run average cost based on N regenerative cycles as

$$\widehat{\mu_\eta^T g} := \frac{1}{\sigma(N)} \sum_{k=0}^{\sigma(N)-1} g(x^{(k)}), \quad (4.2)$$

where $\sigma(n)$ is the n th time when regeneration state x^* is visited. Next, we consider an arbitrary state $x^{(k)}$ from the generated episode. We define a one-replication estimate of the solution to the Poisson equation (4.1) for a state $x^{(k)}$ visited at time k as:

$$\hat{h}_k := \sum_{t=k}^{\sigma_k-1} \left(g(x^{(t)}) - \widehat{\mu_\eta^T g} \right), \quad (4.3)$$

where $\sigma_k = \min \{ t > k \mid x^{(t)} = x^* \}$ is the first time when the regeneration state x^* is visited after time k . We note that the one-replication estimate (4.3) is computed for every timestep. The estimator (4.3) was proposed in [22, Section 5.3].

We use function $f_\psi : \mathcal{X} \rightarrow \mathbb{R}$ from a family of function approximators $\{f_\psi, \psi \in \Psi\}$ to represent function h_η and choose function f_ψ from $\{f_\psi, \psi \in \Psi\}$ to minimize the mean square distance to the one-replication estimates $\{\hat{h}_k\}_{k=0}^{\sigma(N)-1}$:

$$\psi^* = \arg \min_{\psi \in \Psi} \sum_{k=0}^{\sigma(N)-1} \left(f_\psi(x^{(k)}) - \hat{h}_k \right)^2. \quad (4.4)$$

With available function approximation f_{ψ^*} for h_η , we estimate the advantage function (3.16) as:

$$\hat{A}_\eta(x^{(k)}, a^{(k)}) := g(x^{(k)}) - \widehat{\mu_\eta^T g} + \sum_{y \in \mathcal{X}} P(y|x^{(k)}, a^{(k)}) f_{\psi^*}(y) - f_{\psi^*}(x^{(k)}). \quad (4.5)$$

We assume that Q episodes, $Q \geq 1$, can be simulated in parallel, and each of $q = 1, \dots, Q$ (parallel) actors collect an episode

$$\left\{ x^{(0,q)}, a^{(0,q)}, x^{(1,q)}, a^{(1,q)}, \dots, x^{(k,q)}, a^{(k,q)}, \dots, x^{(\sigma^q(N)-1,q)}, a^{(\sigma^q(N)-1,q)} \right\} \quad (4.6)$$

with N regenerative cycles, where $\sigma^q(N)$ is the N th regeneration time in the simulation of q th actor and $x^{(0,q)} = x^*$ for each $q = 1, \dots, Q$. Given the episodes (4.6) generated under policy π_η , we compute the advantage function estimates $\hat{A}_\eta(x^{(k,q)}, a^{(k,q)})$ by (4.5):

$$D^{(0:\sigma^q(N)-1)}_{q=1} = \left\{ \left(x^{(0,q)}, a^{(0,q)}, \hat{A}_\eta(x^{(0,q)}, a^{(0,q)}) \right), \dots, \left(x^{(\sigma^q(N)-1,q)}, a^{(\sigma^q(N)-1,q)}, \hat{A}_\eta(x^{(\sigma^q(N)-1,q)}, a^{(\sigma^q(N)-1,q)}) \right) \right\}_{q=1}^Q.$$

We estimate the loss function (3.18) as a sample average over these $\sum_{q=1}^Q \sigma^q(N)$ data-points:

$$\begin{aligned} \hat{L}(\theta, \theta_i, D^{(1:Q), (0:\sigma^q(N)-1)}) &= \sum_{q=1}^Q \sum_{k=0}^{\sigma^q(N)-1} \max \left[\frac{\pi_\theta(a^{(k,q)}|x^{(k,q)})}{\pi_{\theta_i}(a^{(k,q)}|x^{(k,q)})} \hat{A}_{\theta_i}(x^{(k,q)}, a^{(k,q)}), \right. \\ &\quad \left. \text{clip} \left(\frac{\pi_\theta(a^{(k,q)}|x^{(k,q)})}{\pi_{\theta_i}(a^{(k,q)}|x^{(k,q)})}, 1 - \epsilon, 1 + \epsilon \right) \hat{A}_{\theta_i}(x^{(k,q)}, a^{(k,q)}) \right] \end{aligned} \quad (4.7)$$

Optimization of the loss function yields a new policy for the next iteration.

Algorithm 1: Base proximal policy optimization algorithm for long-run average cost problems

Result: policy π_{θ_I}

- 1 Initialize policy π_{θ_0} ;
- 2 **for** policy iteration $i = 0, 1, \dots, I - 1$ **do**
- 3 **for** actor $q = 1, 2, \dots, Q$ **do**
- 4 Run policy π_{θ_i} until it reaches N th regeneration time on $\sigma^q(N)$ step: collect an episode $\{x^{(0,q)}, a^{(0,q)}, x^{(1,q)}, a^{(1,q)}, \dots, x^{(\sigma^q(N)-1,q)}, a^{(\sigma^q(N)-1,q)}, x^{(\sigma^q(N),q)}\}$;
- 5 **end**
- 6 Compute the average cost estimate $\widehat{\mu_{\theta_i}^T g}$ by (4.2) (utilizing Q episodes) ;
- 7 Compute $\hat{h}_{k,q}$, the estimate of $h_{\theta_i}(x^{(k,q)})$, by (4.3) for each $q = 1, \dots, Q$, $k = 0, \dots, \sigma^q(N) - 1$;
- 8 Update $\psi_i := \psi$, where $\psi \in \Psi$ minimizes $\sum_{q=1}^Q \sum_{k=0}^{\sigma^q(N)-1} (f_{\psi}(x^{(k,q)}) - \hat{h}_{k,q})^2$ following (4.4) ;
- 9 Estimate the advantage functions $\hat{A}_{\theta_i}(x^{(k,q)}, a^{(k,q)})$ using (4.5) for each $q = 1, \dots, Q$, $k = 0, \dots, \sigma^q(N) - 1$:

$$D^{(1:Q), (0:\sigma^q(N)-1)} = \left\{ \left(x^{(0,q)}, a^{(0,q)}, \hat{A}_{0,q} \right), \dots, \left(x^{(\sigma^q(N)-1,q)}, a^{(\sigma^q(N)-1,q)}, \hat{A}_{\sigma^q(N)-1,q} \right) \right\}_{q=1}^Q.$$
- 10 Minimize the surrogate objective function w.r.t. $\theta \in \Theta$:

$$\hat{L} \left(\theta, \theta_i, D^{(1:Q), (0:\sigma^q(N)-1)} \right) = \sum_{q=1}^Q \sum_{k=0}^{\sigma^q(N)-1} \max \left[\frac{\pi_{\theta}(a^{(k,q)} | x^{(k,q)})}{\pi_{\theta_i}(a^{(k,q)} | x^{(k,q)})} \hat{A}_{\theta_i}(x^{(k,q)}, a^{(k,q)}), \right. \\ \left. \text{clip} \left(\frac{\pi_{\theta}(a^{(k,q)} | x^{(k,q)})}{\pi_{\theta_i}(a^{(k,q)} | x^{(k,q)})}, 1 - \epsilon, 1 + \epsilon \right) \hat{A}_{\theta_i}(x^{(k,q)}, a^{(k,q)}) \right]$$
- 11 Update $\theta_{i+1} := \theta$.
- 12 **end**

In practice a naive (standard) Monte Carlo estimator (4.3) fails to improve in PPO policy iteration Algorithm 1 because of the large variance (i.e. the estimator is unreliable). Therefore, we progressively develop a sequence of estimators in the next subsections. We end this section with two remarks.

Remark 3. For any state $x \in \mathcal{X}$ the one-replication estimate (4.3) is computed each time the state is visited (the every-visit Monte-Carlo method). It is also possible to implement a first-visit Monte Carlo method which implies that a one-replication estimate is computed when state x is visited for the first time within a cycle and that the next visits to state x within the same cycle are ignored. See [80, Section 5.1] for more details of every-visit and first-visit Monte-Carlo methods.

Remark 4. In regression problem (4.4), each data point $(x^{(k)}, \hat{h}_k)$ is used in the quadratic loss function, despite that many of the $x^{(k)}$'s represent the same state. It is possible to restrict that only distinct $x^{(k)}$'s are used in the loss function, with corresponding \hat{h}_k 's properly averaged. It turns out that this new optimization problem yields the same optimal solution as the one in (4.4). The equivalence of the optimization problems follows from the fact that for an arbitrary sequence of real numbers $a_1, \dots, a_n \in \mathbb{R}$:

$$\arg \min_{x \in B} \left[\sum_{i=1}^n (x - a_i)^2 \right] = \arg \min_{x \in B} \left[\left(x - \frac{1}{n} \sum_{i=1}^n a_i \right)^2 \right],$$

where B is an arbitrary subset of \mathbb{R} .

4.2 Approximating martingale-process method

Estimator (4.3) of the solution to the Poisson equation suffers from the high variance when the regenerative cycles are long (i.e. the estimator is a sum of many random terms $g(x^{(k)}) - \mu_{\eta}^T g$). In this section we explain how to decrease the variance by reducing the magnitude of summands in (4.3) if an approximation ζ of the solution to Poisson's equation h_{η} is available.

We assume an episode $\{x^{(0)}, a^{(1)}, x^{(1)}, a^{(2)}, \dots, x^{(K-1)}, a^{(K-1)}, x^{(\sigma(N))}\}$ has been generated under policy π_η . From the definition of a solution to the Poisson equation (3.3):

$$g(x^{(k)}) - \mu_\eta^T g = h_\eta(x^{(k)}) - \sum_{y \in \mathcal{X}} P_\eta(y|x^{(k)}) h_\eta(y) \text{ for each state } x^{(k)} \text{ in the simulated episode.}$$

If the approximation ζ is sufficiently close to h_η , then the correlation between

$$g(x^{(k)}) - \widehat{\mu_\eta^T g} \quad \text{and} \quad \zeta(x^{(k)}) - \sum_{y \in \mathcal{X}} P_\eta(y|x^{(k)}) \zeta(y)$$

is positive and we can use the control variate to reduce the variance. This idea gives rise to the approximating martingale-process (AMP) method proposed in [36]; also see [4].

Following [36, Proposition 7], for some approximation ζ such that $\mu_\eta^T \zeta < \infty$ and $\zeta(x^*) = 0$, we consider the martingale process starting from an arbitrary state $x^{(k)}$ until the first regeneration time:

$$M_{\sigma_k}(x^{(k)}) = \zeta(x^{(k)}) + \sum_{t=k}^{\sigma_k-1} \left[\sum_{y \in \mathcal{X}} P_\eta(y|x^{(t)}) \zeta(y) - \zeta(x^{(t)}) \right], \quad (4.8)$$

where $\sigma_k = \min \{t > k \mid x^{(t)} = x^*\}$ is the first time when the regeneration state x^* is visited after time k . The martingale process (4.8) has zero expectation $\mathbb{E}M_n = 0$ for all $n \geq 0$; therefore we use it as a control variate to define a new estimator. Adding M_{σ_k} to estimator (4.3) we get the AMP estimator of the solution to the Poisson equation:

$$\hat{h}_\eta^{AMP(\zeta)}(x^{(k)}) := \zeta(x^{(k)}) + \sum_{t=k}^{\sigma_k-1} \left(g(x^{(t)}) - \widehat{\mu_\eta^T g} + \sum_{y \in \mathcal{X}} P_\eta(y|x^{(t)}) \zeta(y) - \zeta(x^{(t)}) \right). \quad (4.9)$$

We assume that the estimation of the average cost is accurate (i.e. $\widehat{\mu_\eta^T g} = \mu_\eta^T g$). In this case estimator (4.9) has zero variance if the approximation is exact $\zeta = h_\eta$.

Now we want to replace the standard regenerative estimator (4.3) used in line 8 of Algorithm 1 with AMP estimator (4.9). As the approximation ζ needed in (4.9), we use $f_{\psi_{i-1}}$ that approximates a solution to the Poisson equation corresponding to previous policy $\pi_{\theta_{i-1}}$. In line 8 of Algorithm 1 we replace $\hat{h}(x^{(k)})$ with the estimates $\hat{h}^{AMP(f_{\psi_{i-1}})}(x^{(k)})$ that are computed by (4.9).

4.3 Variance reduction through discounting

Unless an approximation ζ is exact, each term in the summation in (4.9) is random with nonzero variance. When the expected length of a regeneration cycle is large, the cumulative variance of estimator (4.9) can be devastating.

In this subsection, we describe a commonly used solution: introduce a forgetting factor $\gamma \in (0, 1)$ to discount the future relative costs, [41, 9, 56, 43, 81, 74].

We let

$$r(x^*) := (1 - \gamma) \mathbb{E} \left[\sum_{t=0}^{\infty} \gamma^t g(x^{(t)}) \mid x^{(0)} = x^* \right] \quad (4.10)$$

be a *present discounted value* at state x^* ; the term ‘‘present discounted value’’ was proposed in [84, Section 11.2]. We define the *regenerative discounted relative value function* as:

$$V^{(\gamma)}(x) := \mathbb{E} \left[\sum_{t=0}^{\sigma(x^*)-1} \gamma^t \left(g(x^{(t)}) - r(x^*) \right) \mid x^{(0)} = x \right] \text{ for each } x \in \mathcal{X}, \quad (4.11)$$

where $x^{(k)}$ is the state of the Markov chain with transition matrix P at time k , x^* is the prespecified regeneration state, and $\gamma \in (0, 1]$ is a discount factor. We note that $V^{(\gamma)}(x^*) = 0$ by definition. It

Algorithm 2: Proximal policy optimization with AMP method

Result: policy π_{θ_I}

- 1 Initialize policy π_{θ_0} and value function $f_{\psi_{-1}} \equiv 0$ approximators ;
 - 2 **for** *policy iteration* $i = 0, 1, \dots, I - 1$ **do**
 - 3 **for** *actor* $q = 1, 2, \dots, Q$ **do**
 - 4 Run policy π_{θ_i} until it reaches N th regeneration time on $\sigma^q(N)$ step: collect an episode
 $\{x^{(0,q)}, a^{(0,q)}, x^{(1,q)}, a^{(1,q)}, \dots, x^{(\sigma^q(N)-1,q)}, a^{(\sigma^q(N)-1,q)}, x^{(\sigma^q(N),q)}\}$;
 - 5 **end**
 - 6 Compute the average cost estimate $\widehat{\mu_{\theta_i}^T g}$ by (4.2);
 - 7 Compute $\hat{h}_{k,q}^{AMP(f_{\psi_{i-1}})}$, the estimate of $h_{\theta_i}(x^{(k,q)})$, by (4.9) for each $q = 1, \dots, Q$,
 $k = 0, \dots, \sigma^q(N) - 1$;
 - 8 Update $\psi_i := \psi$, where $\psi \in \Psi$ minimizes $\sum_{q=1}^Q \sum_{k=0}^{\sigma^q(N)-1} \left(f_{\psi}(x^{(k,q)}) - \hat{h}_{k,q}^{AMP(f_{\psi_{i-1}})} \right)^2$ following
 (4.4);
 - 9 Estimate the advantage functions $\hat{A}_{\theta_i}(x^{(k,q)}, a^{(k,q)})$ using (4.5) for each $q = 1, \dots, Q$,
 $k = 0, \dots, \sigma^q(N) - 1$:

$$D^{(0:\sigma^q(N)-1)}_{q=1}^Q = \left\{ \left(x^{(0,q)}, a^{(0,q)}, \hat{A}_{0,q} \right), \dots, \left(x^{(\sigma^q(N)-1,q)}, a^{(\sigma^q(N)-1,q)}, \hat{A}_{\sigma^q(N)-1,q} \right) \right\}_{q=1}^Q.$$
 - 10 Minimize the surrogate objective function w.r.t. $\theta \in \Theta$:

$$\hat{L} \left(\theta, \theta_i, D^{(0:\sigma^q(N)-1)}_{q=1}^Q \right) = \sum_{q=1}^Q \sum_{k=0}^{\sigma^q(N)-1} \max \left[\frac{\pi_{\theta}(a^{(k,q)}|x^{(k,q)})}{\pi_{\theta_i}(a^{(k,q)}|x^{(k,q)})} \hat{A}_{\theta_i}(x^{(k,q)}, a^{(k,q)}), \right.$$

$$\left. \text{clip} \left(\frac{\pi_{\theta}(a^{(k,q)}|x^{(k,q)})}{\pi_{\theta_i}(a^{(k,q)}|x^{(k,q)})}, 1 - \epsilon, 1 + \epsilon \right) \hat{A}_{\theta_i}(x^{(k,q)}, a^{(k,q)}) \right]$$
 - 11 Update $\theta_{i+1} := \theta$.
 - 12 **end**
 - 13 **end**
-

follows from [70, Corollary 8.2.5.] that under the drift condition, $r(x^*) \rightarrow \mu^T g$ as $\gamma \uparrow 1$. Furthermore, by Lemma 7, for each $x \in \mathcal{X}$,

$$V^{(\gamma)}(x) \rightarrow h^{(x^*)}(x) \text{ as } \gamma \uparrow 1,$$

where $h^{(x^*)}$ is a solution to the Poisson equation given in (4.1).

The proof of Lemma 7 can be found in Appendix Section B.

Lemma 7. *We consider irreducible, aperiodic Markov chain with transition matrix P that satisfies drift condition (3.1). We let (4.11) be a regenerative discounted relative value function for discount factor γ and one-step cost function g , such that $|g(x)| < \mathcal{V}(x)$ for each $x \in \mathcal{X}$. We let $h^{(x^*)}$ be a solution of the Poisson equation (3.3) defined by (4.1).*

Then for some constants $R < \infty$ and $r \in (0, 1)$ we have

$$\left| V^{(\gamma)}(x) - h^{(x^*)}(x) \right| \leq \frac{rR(1-\gamma)}{(1-r)(1-\gamma r)} (\mathcal{V}(x) + \mathcal{V}(x^*))$$

for each $x \in \mathcal{X}$.

We let

$$\hat{V}^{(\gamma)}(x) := \sum_{k=0}^{\sigma(x^*)-1} \gamma^k \left(g(x^{(k)}) - r(x^*) \right) \quad (4.12)$$

where $x^{(0)} = x$ and $x^{(k)}$ is the k th step of the Markov chain with transition matrix P , be an one-replication estimate of (4.11). By Lemma 8 the variance of this estimator $\text{Var}[\hat{V}^{(\gamma)}(x)]$ converges to zero with rate γ^2 as $\gamma \downarrow 0$ for each $x \in \mathcal{X}$. See Appendix Section B for the proof.

Lemma 8. *We consider irreducible, aperiodic Markov chain with transition matrix P that satisfies drift condition (3.1) and assume that one-step cost function $g : \mathcal{X} \rightarrow \mathbb{R}$ satisfies $g^2(x) \leq \mathcal{V}(x)$ for each $x \in \mathcal{X}$. We let (4.11) be a regenerative discounted relative value function for discount factor γ , and assume that regeneration state x^* is such that set*

$$\left\{ x \in \mathcal{X} : b\mathcal{V}(x) \leq \mathcal{V}(x^*) \right\}$$

is a finite set, where function \mathcal{V} and constant b are from (3.1). We consider an arbitrary $x \in \mathcal{X}$ and let (4.12) be an one-replication estimate of (4.11).

If $\gamma < 1$, then there exist constants $R < \infty$, $B < \infty$, and $r \in (0, 1)$ independent of γ such that the variance of estimate (4.12) is bounded as

$$\text{Var}[\hat{V}^{(\gamma)}(x)] \leq \gamma^2 \left(R\mathcal{V}(x) \frac{1}{1 - \gamma^2 r} + (\mu^T \mathcal{V}) B \frac{1}{1 - \gamma^2} \right), \text{ for each } x \in \mathcal{X},$$

where μ is a stationary distribution of transition matrix P .

For a fixed $\gamma \in (0, 1)$ and state $x \in \mathcal{X}$ any unbiased estimator of $V^{(\gamma)}(x)$ is a biased estimator of $h^{(x^*)}(x)$. It turns out that the discount counterparts of the estimators (4.3) and (4.9) for $V^{(\gamma)}(x)$ have smaller variances than the two estimators for $h^{(x^*)}(x)$. This variance reduction can be explained intuitively as follows. Introducing the discount factor γ can be interpreted as a modification of the original transition dynamics; under the modified dynamics, any action produces a transition into a regeneration state with probability at least $1 - \gamma$, thus shortening the length of regenerative cycles. See Appendix Section B for details.

We define a *discounted* advantage function for policy π_η as:

$$A_\eta^{(\gamma)}(x, a) := \mathbb{E}_{y \sim P(\cdot|x, a)} \left[g(x) - \mu_\eta^T g + V_\eta^{(\gamma)}(y) - V_\eta^{(\gamma)}(x) \right]. \quad (4.13)$$

For two policies π_θ and π_η , $\eta, \theta \in \Theta$, we define an approximation of $N_1(\theta, \eta)$ (3.15) as:

$$N_1^{(\gamma)}(\theta, \eta) := \mathbb{E}_{\substack{x \sim \mu_\eta \\ a \sim \pi_\theta(\cdot|x)}} \left[r_{\theta, \eta}(a|x) A_\eta^{(\gamma)}(x, a) \right]. \quad (4.14)$$

We use the function approximation f_ψ of $V_\eta^{(\gamma)}$ to estimate the advantage function (4.13) as (4.5).

We now present the discounted version of the AMP estimator (4.9). We let ζ be an approximation of the discounted value function $V_\eta^{(\gamma)}$ such that $\mu_\eta^T \zeta < \infty$ and $\zeta(x^*) = 0$. We define the sequence $(M_\eta^{(n)} : n \geq 0)$:

$$M_\eta^{(n)}(x) := \sum_{t=k}^{n-1} \gamma^{t-k+1} \left[\zeta(x^{(t+1)}) - \sum_{y \in \mathcal{X}} P_\eta(y|x^{(t)}) \zeta(y) \right], \quad (4.15)$$

where $x = x^{(k)}$ and $x^{(t)}$ is a state of the Markov chain after t steps.

We define a one-replication of the AMP estimator for the discounted value function:

$$\begin{aligned} \hat{V}_\eta^{AMP(\zeta), (\gamma)}(x^{(k)}) &:= \sum_{t=k}^{\sigma_k-1} \gamma^{t-k} \left(g(x^{(t)}) - \widehat{r_\eta(x^*)} \right) - M_\eta^{(\sigma_k)}(x^{(k)}) \\ &= \zeta(x^{(k)}) + \sum_{t=k}^{\sigma_k-1} \gamma^{t-k} \left(g(x^{(t)}) - \widehat{r_\eta(x^*)} + \gamma \sum_{y \in \mathcal{X}} P_\eta(y|x^{(t)}) \zeta(y) - \zeta(x^{(t)}) \right) - \gamma^{\sigma_k-k} \zeta(x^*) \\ &= \zeta(x^{(k)}) + \sum_{t=k}^{\sigma_k-1} \gamma^{t-k} \left(g(x^{(t)}) - \widehat{r_\eta(x^*)} + \gamma \sum_{y \in \mathcal{X}} P_\eta(y|x^{(t)}) \zeta(y) - \zeta(x^{(t)}) \right), \end{aligned} \quad (4.16)$$

where $\widehat{r_\eta}(x^*)$ is an estimation of $r(x^*)$, and $\sigma_k = \min \{t > k \mid x^{(t)} = x^*\}$ is the first time the regeneration state x^* is visited after time k .

The AMP estimator (4.20) does not introduce any bias subtracting M_η from $\widehat{V}_\eta^{(\gamma)}$ since $\mathbb{E}M_\eta^{(n)} = 0$ for any $n > 0$ by [36]. Function $V_\eta^{(\gamma)}$ is a solution of the following equation (see Lemma 10):

$$g(x) - r_\eta(x^*) + \gamma \sum_{y \in \mathcal{X}} P_\eta(y|x)h(y) - h(x) = 0 \quad \text{for each } x \in \mathcal{X}. \quad (4.17)$$

Therefore, similar to (4.9), estimator (4.20) has zero variance if approximation is exact $\widehat{r_\eta}(x^*) = r_\eta(x^*)$ and $\zeta = V_\eta$, see Poisson equation (4.17).

Further variance reduction is possible via *T-step truncation* [80, Section 6]. We consider an estimate of the value function (4.11) at a state $x \in \mathcal{X}$ as the sum of the discounted costs before time T , where $T < \sigma(x^*)$, and the discounted costs after time T :

$$\widehat{V}^{(\gamma)}(x) = \sum_{t=0}^{T-1} \gamma^t \left(g(x^{(t)}) - \widehat{r}(x^*) \right) + \gamma^T \sum_{t=0}^{\sigma(x^*)-1} \gamma^t \left(g(x^{(T+t)}) - \widehat{r}(x^*) \right), \quad (4.18)$$

where $x^{(0)} = x$, $x^{(t)}$ is a state of the Markov chain after t steps and $\sum_{t=0}^{\sigma(x^*)-1} \gamma^t g(x^{(T+t)})$ is a standard one-replication estimation of the value function at state $x^{(T)}$. Instead of estimating the value at state $x^{(T)}$ by a random roll-out (second term in (4.18)), we can use the value of deterministic approximation function ζ at state $x^{(T)}$. The T -step truncation reduces the variance of the standard estimator but introduces bias unless the approximation is exact $\zeta(x^{(T)}) = V^{(\gamma)}(x^{(T)})$.

A T -truncated version of the AMP estimator is

$$\begin{aligned} \widehat{V}_k^{AMP(\zeta),(\gamma,T)} &:= \sum_{t=k}^{T \wedge \sigma_k - 1} \gamma^{t-k} \left(g(x^{(t)}) - \widehat{r_\eta}(x^*) \right) + \gamma^{T \wedge \sigma_k - k} \zeta(x^{(T \wedge \sigma_k)}) - M_\eta^{(T \wedge \sigma_k)}(x^{(k)}) \\ &= \sum_{t=k}^{T \wedge \sigma_k - 1} \gamma^{t-k} \left(g(x^{(t)}) - \widehat{r_\eta}(x^*) \right) - \sum_{t=k}^{T \wedge \sigma_k - 1} \gamma^{t-k+1} \left(\zeta(x^{(t+1)}) - \sum_{y \in \mathcal{X}} P_\eta(y|x^{(t)}) \zeta(y) \right) \\ &\quad + \gamma^{T \wedge \sigma_k - k} \zeta(x^{(T \wedge \sigma_k)}) \\ &= \zeta(x^{(k)}) + \sum_{t=k}^{T \wedge \sigma_k - 1} \gamma^{t-k} \left(g(x^{(t)}) - \widehat{r_\eta}(x^*) + \gamma \sum_{y \in \mathcal{X}} P_\eta(y|x^{(t)}) \zeta(y) - \zeta(x^{(t)}) \right), \end{aligned} \quad (4.19)$$

where $T \wedge \sigma_k = \min(T, \sigma_k)$. We note that if the value function approximation and present discounted value approximation are exact, estimator (4.19) is unbiased for $V^{(\gamma)}(x^{(k)})$ and has zero variance. We generalize the T -truncated estimator by taking the number of summands T to follow the geometrical distribution with parameter $\lambda < 1$ as in the TD(λ) method [80, Section 12], [74, Section 3]:

$$\begin{aligned} \widehat{V}_k^{AMP(\zeta),(\gamma,\lambda)} &:= \mathbb{E}_{T \sim \text{Geom}(1-\lambda)} \widehat{V}_k^{AMP(\zeta),(\gamma,T)} \\ &= (1-\lambda) \left(\widehat{V}_k^{AMP(\zeta),(\gamma,1)} + \lambda \widehat{V}_k^{AMP(\zeta),(\gamma,2)} + \lambda^2 \widehat{V}_k^{AMP(\zeta),(\gamma,3)} + \dots \right. \\ &\quad \left. + \lambda^{\sigma_k} \widehat{V}_k^{AMP(\zeta),(\gamma,\sigma_k)} + \lambda^{\sigma_k+1} \widehat{V}_k^{AMP(\zeta),(\gamma,\sigma_k)} + \dots \right) \\ &= \zeta(x^{(k)}) + \sum_{t=k}^{\sigma_k-1} (\gamma\lambda)^{t-k} \left(g(x^{(t)}) - \widehat{r_\eta}(x^*) + \gamma \sum_{y \in \mathcal{X}} P_\eta(y|x^{(t)}) \zeta(y) - \zeta(x^{(t)}) \right). \end{aligned} \quad (4.20)$$

The regenerative cycles can be very long. In practice we want to control/predict the time and memory amount allocated for the algorithm execution. Therefore, the simulated episodes should have finite lengths. We use the following estimation for the first N timesteps if an episode with finite length $N + L$ is generated:

$$\widehat{V}_k^{AMP(\zeta),(\gamma,\lambda,N+L)} := \zeta(x^{(k)}) + \sum_{t=k}^{(N+L) \wedge \sigma_k - 1} (\gamma\lambda)^{t-k} \left(g(x^{(t)}) - \widehat{r_\eta}(x^*) + \gamma \sum_{y \in \mathcal{X}} P_\eta(y|x^{(t)}) \zeta(y) - \zeta(x^{(t)}) \right), \quad (4.21)$$

where $k = 0, \dots, N - 1$, and integer L is large enough. We note that if an episode has a finite length $N + L$, regeneration σ_k may have not been observed in the generated episode (i.e. $\sigma_k > N + L$). In this case, we summarize (4.21) up to the end of the episode.

We provide the PPO algorithm where each of $q = 1, \dots, Q$ parallel actors simulates an episode with length $N + L$: $\{x^{(0,q)}, a^{(0,q)}, x^{(1,q)}, a^{(1,q)}, \dots, x^{(N+L-1,q)}, a^{(N+L-1,q)}\}$. Since we need the approximation ζ in (4.21), we use $f_{\psi_{i-1}}$ that approximates a regenerative discounted value function corresponding to previous policy $\pi_{\theta_{i-1}}$. See Algorithm 3.

Algorithm 3: Proximal policy optimization with discounting

Result: policy π_{θ_I}

1 Initialize policy π_{θ_0} and value function $f_{\psi_{-1}} \equiv 0$ approximators ;

2 **for** policy iteration $i = 0, 1, \dots, I - 1$ **do**

3 **for** actor $q = 1, 2, \dots, Q$ **do**

4 Run policy π_{θ_i} for $N + L$ timesteps: collect an episode
 $\{x^{(0,q)}, a^{(0,q)}, x^{(1,q)}, a^{(1,q)}, \dots, x^{(N+L-1,q)}, a^{(N+L-1,q)}\}$;

5 **end**

6 Estimate the average cost $\widehat{\mu_{\theta_i}^T g}$ by (4.2), the present discounted value $\widehat{r_{\theta_i}(x^*)}$ by (4.22) below;

7 Compute $\widehat{V}_{k,q}^{AMP(f_{\psi_{i-1}}),(\gamma,\lambda)}$ estimates by (4.21) for each $q = 1, \dots, Q$, $k = 0, \dots, N - 1$;

8 Update $\psi_i := \psi$, where $\psi \in \Psi$ minimizes $\sum_{q=1}^Q \sum_{k=0}^{N-1} \left(f_{\psi}(x^{(k,q)}) - \widehat{V}_{k,q}^{AMP(f_{\psi_{i-1}}),(\gamma,\lambda)} \right)^2$ following (4.4) ;

9 Estimate the advantage functions $\hat{A}_{\theta_i}(x^{(k,q)}, a^{(k,q)})$ using (4.5) for each $q = 1, \dots, Q$, $k = 0, \dots, N - 1$:

10
$$D^{(0:N-1)}_{q=1} = \left\{ \left(x^{(0,q)}, a^{(0,q)}, \hat{A}_{\theta_i}^{(\gamma)}(x^{(0,q)}, a^{(0,q)}) \right), \dots, \left(x^{(N-1,q)}, a^{(N-1,q)}, \hat{A}_{\theta_i}^{(\gamma)}(x^{(N-1,q)}, a^{(N-1,q)}) \right) \right\}_{q=1}^Q$$

11 Minimize the surrogate objective function w.r.t. $\theta \in \Theta$:

$$\hat{L}^{(\gamma)}(\theta, \theta_i, D^{(0:N-1)}_{q=1}) = \sum_{q=1}^Q \sum_{k=0}^{N-1} \max \left[\frac{\pi_{\theta}(a^{(k,q)} | x^{(k,q)})}{\pi_{\theta_i}(a^{(k,q)} | x^{(k,q)})} \hat{A}_{\theta_i}^{(\gamma)}(x^{(k,q)}, a^{(k,q)}), \right. \\ \left. \text{clip} \left(\frac{\pi_{\theta}(a^{(k,q)} | x^{(k,q)})}{\pi_{\theta_i}(a^{(k,q)} | x^{(k,q)})}, 1 - \epsilon, 1 + \epsilon \right) \hat{A}_{\theta_i}^{(\gamma)}(x^{(k,q)}, a^{(k,q)}) \right];$$

12 Update $\theta_{i+1} := \theta$.

13 **end**

In Algorithm 3, we assume that state x^* has been visited N_q times in the q th generated episode, when $q = 1, \dots, Q$ parallel actors are available. Therefore, we estimate the present discounted value $r(x^*)$ as:

$$\widehat{r(x^*)} = (1 - \gamma) \frac{1}{\sum_{q=1}^Q N_q} \sum_{q=1}^Q \sum_{n=1}^{N_q} \sum_{k=\sigma^q(n)}^{\sigma^q(n)+L} \gamma^{k-\sigma^q(n)} g(x^{(k,q)}), \quad (4.22)$$

where $\sigma^q(n)$ is the n th time when state x^* is visited in the q th episode, and integer L is a large enough. If many parallel actors are available, we recommend starting the episodes from state x^* to ensure that state x^* appears in the generated episodes a sufficient number of times.

Remark 5. Use the following discounted value function as an approximation of the solution h_{η} of the Poisson equation:

$$J^{(\gamma)}(x) := \mathbb{E} \left[\sum_{k=0}^{\infty} \gamma^k \left(g(x^{(k)}) - \mu^T g \right) \mid x^{(0)} = x \right] \text{ for each } x \in \mathcal{X}. \quad (4.23)$$

We note that the discounted value function (4.23) and the regenerative discounted value function (4.11) are solutions of the same Poisson equation (Lemma B.2). Therefore, the bias of advantage function estimator (4.13) does not change when h_{η} in (3.16) is replaced either by $J^{(\gamma)}$ or by $V^{(\gamma)}$. The variance

of the regenerative discounted value function estimator (4.21) can be potentially smaller than the variance of the analogous $J^{AMP(\zeta),(\gamma,\lambda,N+L)}$ estimator:

$$\hat{j}_k^{AMP(\zeta),(\gamma,\lambda,N+L)} := \zeta(x^{(k)}) + \sum_{t=k}^{N+L-1} (\gamma\lambda)^{t-k} \left(g(x^{(t)}) - \widehat{\mu}_\eta^T g + \gamma \sum_{y \in \mathcal{X}} P_\eta(y|x^{(t)}) \zeta(y) - \zeta(x^{(t)}) \right). \quad (4.24)$$

Since the upper bound of summation in (4.21) is $\min(\sigma_k, N+L) - 1$, it includes fewer summands than the summation in (4.24) if the regeneration frequently occurs. See Appendix Section D, which describes a numerical experiment for the criss-cross network implying that the choice of $J^{AMP(\zeta),(\gamma,\lambda,N+L)}$ and $V^{AMP(\zeta),(\gamma,\lambda,N+L)}$ estimators can affect the PPO algorithm convergence rate to the optimal policy.

The connection between our proposed AMP estimator and the GAE estimator [74] suggests another motivation for introducing the GAE estimator. An accurate estimation of the value function $V_\eta^{(\gamma)}$ by the standard estimator may require a large number of state-action pairs samples from the current policy π_η [80, Section 13], [74, 40]. In this paper we apply the AMP method to propose the discounted AMP estimator in (4.21) that has a smaller variance than the estimators (4.18). The AMP method, however, requires knowledge of transition probabilities $P(y|x, a)$ in order to exactly compute the expected values for each $(x, a, y) \in \mathcal{X} \times \mathcal{A} \times \mathcal{X}$:

$$\mathbb{E}_{\substack{a \sim \pi_\eta(\cdot|x) \\ y \sim P(\cdot|x,a)}} \zeta(y) = \sum_{y \in \mathcal{X}} \sum_{a \in \mathcal{A}} P(y|x, a) \pi_\eta(a|x) \zeta(y).$$

One can relax the requirement by replacing each expected value $\mathbb{E}_{\substack{a \sim \pi_\eta(\cdot|x^{(t)}) \\ y \sim P(\cdot|x,a)}} \zeta(y)$ by its *one-replication estimate* $\zeta(x^{(t+1)})$, where $(x^{(t)}, x^{(t+1)})$ are two sequential states from an episode

$$(x^{(0)}, \dots, x^{(t)}, x^{(t+1)}, \dots)$$

generated under policy π_η .

In Section 4.3 we propose the AMP estimator of the regenerative discounted value function (4.20):

$$\hat{V}_k^{AMP(\zeta),(\gamma,\lambda)} = \zeta(x^{(k)}) + \sum_{t=k}^{\sigma_k-1} (\gamma\lambda)^{t-k} \left(g(x^{(t)}) - \widehat{r}(x^*) + \gamma \sum_{y \in \mathcal{X}} P_\eta(y|x^{(t)}) \zeta(y) - \zeta(x^{(t)}) \right). \quad (4.25)$$

Replacing expectations $\sum_{y \in \mathcal{X}} P_\eta(y|x^{(t)}) \zeta(y)$ by the one-replication estimates $\zeta(x^{(t+1)})$ we obtain the following estimator for the value function:

$$\hat{V}_k^{GAE(\zeta),(\gamma,\lambda)} := \zeta(x^{(k)}) + \sum_{t=k}^{\sigma_k-1} (\gamma\lambda)^{t-k} \left(g(x^{(k+t)}) - \widehat{r}(x^*) + \gamma \zeta(x^{(t+1)}) - \zeta(x^{(t)}) \right), \quad (4.26)$$

which is a part of the general advantage estimation (GAE) method [74]. We note that the advantage function is estimated as $\hat{A}_k^{GAE(\zeta),(\gamma,\lambda)} := \hat{V}_k^{GAE(\zeta),(\gamma,\lambda)} - \zeta(x^{(k)})$ in [74].

If $\lambda = 1$, the estimator (4.20) is transformed into the standard estimator and does not depend on ζ :

$$\begin{aligned} \hat{V}_\eta^{(\zeta),(\gamma)}(x^{(k)}) &:= \zeta(x^{(k)}) + \sum_{t=k}^{\sigma_k-1} \gamma^{t-k} \left(g(x^{(t)}) - \widehat{r}(x^*) + \gamma \zeta(x^{(t+1)}) - \zeta(x^{(t)}) \right) \\ &= \sum_{t=k}^{\sigma_k-1} \gamma^{t-k} \left(g(x^{(t)}) - \widehat{r}(x^*) \right). \end{aligned}$$

The martingale-based control variate has no effect on the GAE estimator when $\lambda = 1$, but it can produce significant variance reductions in the AMP estimator. See Section 5.1 for numerical experiments.

5 Experimental results for multiclass queueing networks

In this section we evaluate the performance of the proposed proximal policy optimization Algorithms 1, 2, and 3 for the multiclass queueing networks control optimization task discussed in Section 2.

We use two separate fully connected feed-forward neural networks to represent policies π_θ , $\theta \in \Theta$ and value functions f_ψ , $\psi \in \Psi$ with the architecture details given in Appendix Section E. We refer to the neural network used to represent a policy as *the policy NN* and to the neural network used to approximate a value function as *the value function NN*. We run the algorithm for $I = 200$ policy iterations for each experiment. The algorithm uses $Q = 50$ actors to simulate data in parallel for each iteration. See Appendix Section F for the details.

5.1 Criss-cross network

We first study the PPO algorithm and compare its base version Algorithm 1 and its modification Algorithm 2 that incorporates the AMP method. We check the robustness of the algorithms for the criss-cross system with various load (traffic) intensity regimes, including I.L. (imbalanced light), B.L. (balanced light), I.M. (imbalanced medium), B.M. (balanced medium), I.H. (imbalanced heavy), and B.H. (balanced heavy) regimes. Table 1 lists the corresponding arrival and service rates. The criss-cross network in any of these traffic regimes is stable under any work-conserving policy [23]. Since we want an initial policy to be stable, we forbid each server in the network to idle unless all its associated buffers are empty.

Table 2 summarizes the control policies proposed in the literature. Column 1 reports the load regimes, column 2 reports the optimal performance obtained by dynamic programming (DP), column 3 reports the performance of a target-pursuing policy (TP) [67], column 4 reports the performance of a threshold policy [35], columns 5 and 6 report the performance of fluid (FP) and robust fluid (RFP) policies respectively [14], and column 7 reports the performance and the half width of the 95% confidence intervals (CIs) of the PPO policy π_{θ_i} resulting from the last iteration of Algorithm 2.

We initialize the policy NN parameters θ_0 using standard Xavier initialization [27]. The resulting policy π_{θ_0} is close to the policy that chooses actions uniformly at random. We take the empty system state $x^* = (0, 0, 0)$ as a regeneration state and simulate $N = 5,000$ independent regenerative cycles per actor in each iteration of the algorithm. Although the number of generated cycles is fixed for all traffic regimes, the length of the regenerative cycles varies and highly depends on the load.

To show the learning curves in Figure 2, we save policy parameters $\{\theta_i\}_{i=0,10,\dots,200}$ every 10th iteration over the course of learning. After the algorithm terminates we independently simulate policies $\{\pi_{\theta_i} : i = 0, 10, \dots, 200\}$ (in parallel) starting from the regeneration state $x = (0, \dots, 0)$ until a fixed number of regenerative events occurs. For light, medium, and heavy traffic regimes, we run the simulations for 5×10^7 , 5×10^6 , and 10^6 regenerative cycles respectively. We compute the 95%–confidence intervals using the strongly consistent estimator of asymptotic variance. See [5, Section VI.2d].

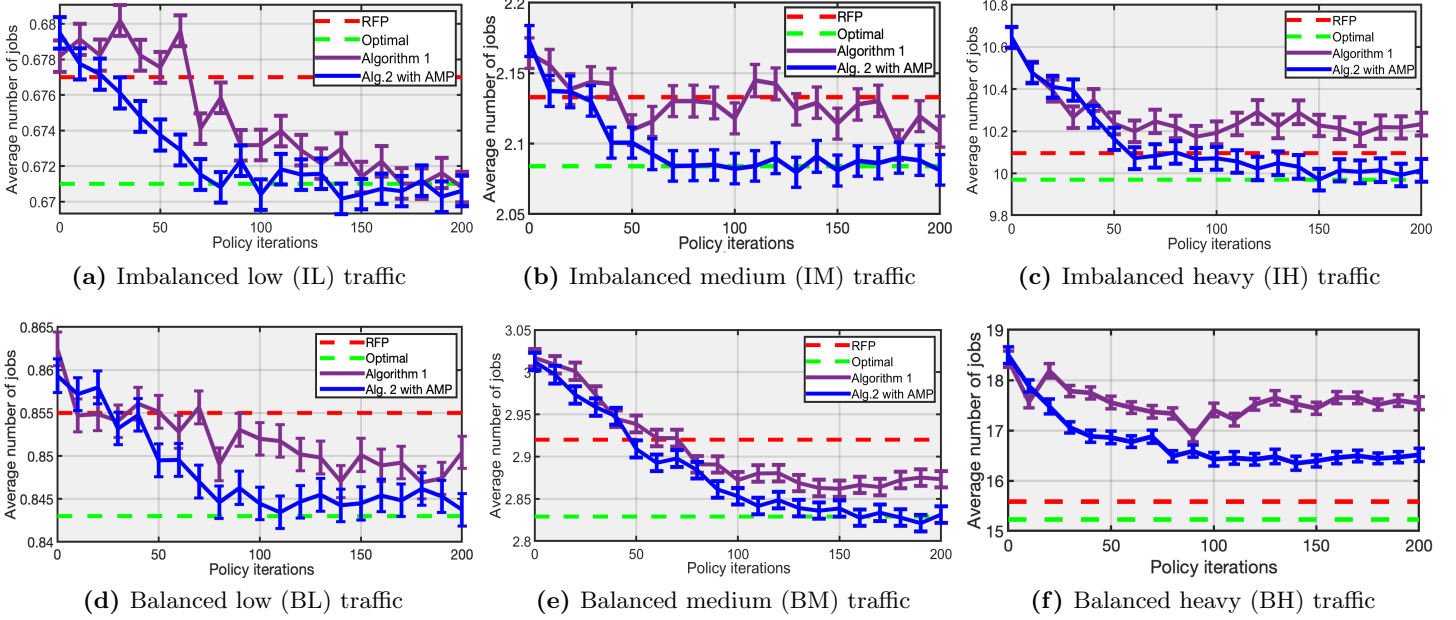


Figure 2: Comparison of learning curves from Algorithm 1 and Algorithm 2 on the criss-cross network with different traffic regimes. The solid purple and blue lines show the performance of the PPO policies obtained at the end of every 10th iterations of Algorithm 1 and Algorithm 2, respectively; the dashed red lines show the performance of the robust fluid policy (RFP), and the dashed green lines show the performance of the optimal policy.

Load regime	λ_1	λ_3	μ_1	μ_2	μ_3	ρ_1	ρ_2
I.L.	0.3	0.3	2	1.5	2	0.3	0.2
B.L.	0.3	0.3	2	1	2	0.3	0.3
I.M.	0.6	0.6	2	1.5	2	0.6	0.4
B.M.	0.6	0.6	2	1	2	0.6	0.6
I.H.	0.9	0.9	2	1.5	2	0.9	0.6
B.H.	0.9	0.9	2	1	2	0.9	0.9

Table 1: Load parameters for the criss-cross network of Figure 1

Load regime	DP (optimal)	TP	threshold	FP	RFP	PPO (Algorithm 2) with CIs
I.L.	0.671	0.678	0.679	0.678	0.677	0.671 ± 0.001
B.L.	0.843	0.856	0.857	0.857	0.855	0.844 ± 0.004
I.M.	2.084	2.117	2.129	2.162	2.133	2.084 ± 0.011
B.M.	2.829	2.895	2.895	2.965	2.920	2.833 ± 0.010
I.H.	9.970	10.13	10.15	10.398	10.096	10.014 ± 0.055
B.H.	15.228	15.5	15.5	18.430	15.585	16.513 ± 0.140

Table 2: Average number of jobs per unit time in the criss-cross network under different policies. Column 1 reports the variances in the load regimes.

We observe that Algorithm 2 is not robust enough and converges to a suboptimal policy when the criss-cross network operates in a balanced heavy load regime. We run Algorithm 3 that uses discount factor $\gamma = 0.998$, TD parameter $\lambda = 0.99$, and the AMP method for the value function estimation at step 7. For each iteration we use $Q = 50$ parallel processes to generate trajectories, each with length $N = 50,000$. We observe that Algorithm 3 uses approximately 10 times fewer samples per iteration than Algorithm 2. Algorithm 3 outputs policy $\pi_{\theta_{200}}$ whose long-run average performance is 15.353 ± 0.138

jobs, which is lower than the RFP performance in [14]. We repeat the experiment with Algorithm 3 with the discounting, but we disable the AMP method in the value function estimation at step 7. Figure 3 shows that both variance reduction techniques (i.e. discounting, AMP method) have been necessary in Algorithm 3 to achieve near-optimal performance.

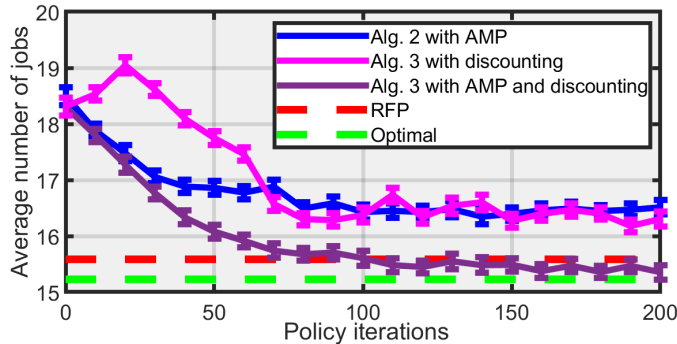


Figure 3: Comparison of learning curves from Algorithm 2 and Algorithm 3 on the criss-cross network with the balanced heavy regime. The solid blue and purple lines show the performance of the PPO policies obtained at the end of every 10th iterations of Algorithm 2 and Algorithm 3, respectively. The solid pink line shows the performance of the PPO policies obtained at the end of every 10th iterations of Algorithm 3 without the AMP method. The dashed red line shows the performance of the robust fluid policy (RFP), and the dashed green line shows the performance of the optimal policy.

Recall that in the uniformization procedure, the transition matrix \tilde{P} in (2.5) allows “fictitious” transitions when $\tilde{P}(x|x) > 0$ for some state $x \in \mathcal{X}$. The PPO algorithm approximately solves the discrete-time MDP (2.12), which allows a decision at every state transition, including fictitious ones. The algorithm produces randomized stationary Markovian policies. In evaluating the performance of any such policies, we actually simulate a DTMC $\{x^{(k)} : k = 0, 1, 2, \dots\}$ operating under the policy, estimating the corresponding long-run average cost as in (2.12). There are two versions of DTMCs depending on how often the randomized policy is sampled to determine the next action. In version 1, the policy is re-sampled only when a *real* state transition occurs. Thus, whenever a fictitious state transition occurs, no new action is determined and server priorities do not change in this version. In version 2, the policy is re-sampled at *every* transition. Unfortunately, there is no guarantee that these two versions of DTMCs yield the same long-run average cost. See [15, Example 2.2] for a counterexample.

When the randomized stationary Markovian policy is optimal for the discrete-time MDP (2.12), under an additional mild condition, the two DTMC versions yield the same long-run average cost [15, Theorem 3.6]. Whenever simulation is used to estimate the performance of a randomized policy in this paper, we use version 1 of the DTMC. The reason for this choice is that the long-run average for this version of DTMC is the same as the continuous-time long-run average cost in (2.11), and the latter performance has been used as benchmarks in literature. Although the final randomized stationary Markovian policy from our PPO algorithm is not expected to be optimal, our numerical experiments demonstrate that the performance results of the DTMC versions 1 and 2 are statistically identical. Table 3 reports the performance of the DTMC versions 1 and 2 in the criss-cross network. In Table column 2, the performance of Version 1 is identical to Table 2 column 7.

Load regime	Version 1 performance with CIs	Version 2 performance with CIs
I.L.	0.671 ± 0.001	0.671 ± 0.001
B.L.	0.844 ± 0.004	0.844 ± 0.004
I.M.	2.084 ± 0.011	2.085 ± 0.011
B.M.	2.833 ± 0.010	2.832 ± 0.010
I.H.	10.014 ± 0.055	9.998 ± 0.054
B.H.	16.513 ± 0.140	16.480 ± 0.137

Table 3: Average number of jobs per unit time in the discrete-time MDP model of the criss-cross network under PPO policies.

5.2 Extended six-class queueing network

In this subsection, we consider the family of extended six-class networks from [14] and apply Algorithm 3 to find good control policies.

Figure 4 shows the structures of the extended six-class networks. We run experiments for 6 different extended six-class queueing networks with the following traffic parameters: $\lambda_1 = \lambda_3 = 9/140$, the service times are exponentially distributed with service rates determined by the modulus after dividing the class index by 6 (i.e. classes associated with server 1 are served with rates $\mu_1 = 1/8, \mu_2 = 1/2, \mu_3 = 1/4$ and classes associated with server 2 are processed with service rates $\mu_4 = 1/6, \mu_5 = 1/7, \mu_6 = 1$). The service rates for the odd servers $S_1, \dots, S_{\lfloor L/2 \rfloor + 1}$ are the same as the service rates for server 1, while the service rates for the even servers $S_2, \dots, S_{\lfloor L/2 \rfloor}$ are the same as the service rates for server 2. The load is the same for each station and is equal to $\rho = 0.9$.

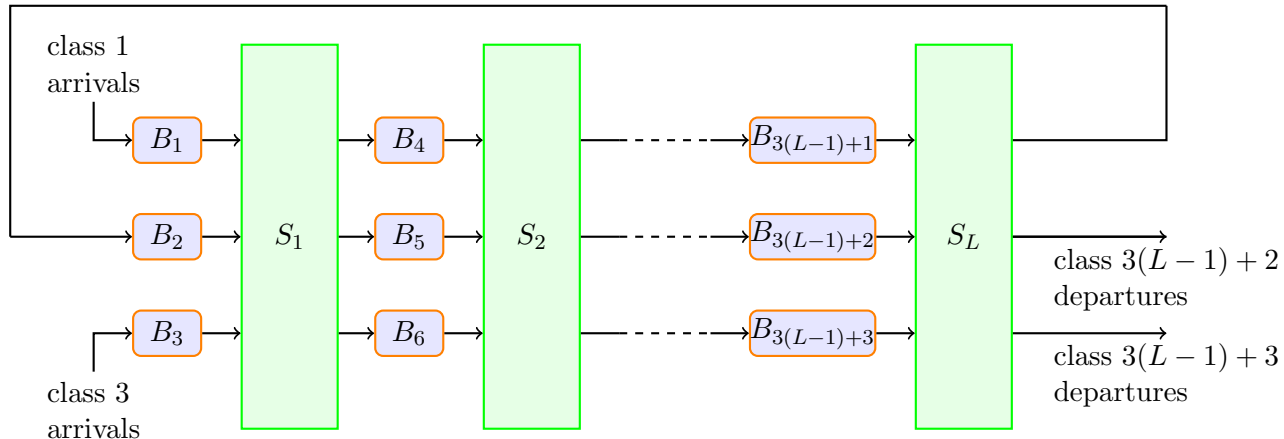


Figure 4: The extended six-class queueing network.

No. of classes $3L$	LBFS	FCFS	FP	RFP	PPO (Algorithm 3) with CIs
6	15.749	40.173	15.422	15.286	14.130 ± 0.208
9	25.257	71.518	26.140	24.917	23.269 ± 0.251
12	34.660	114.860	38.085	36.857	32.171 ± 0.556
15	45.110	157.556	45.962	43.628	39.300 ± 0.612
18	55.724	203.418	56.857	52.980	51.472 ± 0.973
21	65.980	251.657	64.713	59.051	55.124 ± 1.807

Table 4: Numerical results for the extended six-class queueing network in Figure 4.

We vary the size of the network between 6 and 21 classes to test the robustness of the PPO policies. In all experiments we generate $Q = 50$ episodes with $N = 50,000$ timesteps. Table 7 in Appendix Section F reports the running time of the algorithm depending on the size of the queueing network. We set the discount factor and TD parameter to $\gamma = 0.998$ and $\lambda = 0.99$, respectively. Table 4 shows the performance of the PPO policy and compares it with other heuristic methods for the extended six-class queueing networks. In the table FP and RFP refer to fluid and robust fluid policies [14]. Table 4 reports the performance of the best RFP corresponding to the best choice of policy parameters for each class. LBFS refers to the last-buffer first-serve policy, where the priority at a server is given to jobs with highest index. FCFS refers to the first-come first-serve policy, where the priority at a server is given to jobs with the longest waiting time for service.

For each extended six-class network we consider a corresponding discrete-time MDP. We fix a stable, randomized policy for the discrete-time MDP, since the use of Xavier initialization could yield an unstable NN policy for extended six-class networks. We refer to this stable, randomized policy as an expert policy. We simulate a long episode of the MDP operating under the expert policy. At each timestep we save the state at the time and the corresponding probability distribution over the actions. We use this simulated

data set to train the initial NN policy π_{θ_0} . In our numerical experiments, we use the *proportionally randomized (PR)* policy as the expert policy. If the network operates under the PR policy, when an arrival or service completion event occurs at station k , a nonempty buffer j receives a priority over other classes at the station with probability

$$\frac{x_j}{\sum_{i \in \mathcal{B}(k)} x_i}, \quad (5.1)$$

where $\mathcal{B}(k)$ is a set of buffers associated with server k and $x = (x_1, \dots, x_J)$ is the vector of jobcounts at the time of the event after accounting for job arrivals and departures. The priority stays fixed until the next arrival or service completion event occurs. The PR policy is maximally stable for open MQNs, meaning that if the system is unstable under the PR policy, no other policy can stabilize it. See Appendix Section C for the details. An initial NN policy for PPO algorithm plays an important role in its learning process. PPO algorithm may suffer from an exploration issue when the initial NN policy is sufficiently far from the optimal one [85].

In each plot in Figure 5, we save policy NN parameters $\{\theta_i\}_{i=0,10,\dots,200}$ every 10th policy iteration. For each saved policy NN, we conduct a separate long simulation of the queueing network operating under the policy for accurate performance evaluation by providing a 95% confidence interval of the long-run average cost. For any of the six queueing networks, when the load is high, the regeneration is rare. Thus, we adopt the *batch means* method to estimate the confidence interval [37, Section 6]. For each policy from the set $\{\pi_{\theta_i} : i = 0, 10, \dots, 200\}$, we simulate an episode starting from an empty state $x = (0, \dots, 0)$ until 5×10^6 arrival events occur. Then we estimate average performance of the policy based on this episode. To compute the confidence interval from the episode, we split the episode into 50 sub-episodes (batches), see also [65]. Pretending that the obtained 50 mean estimates are i.i.d., we compute the 95%–confidence intervals as shown in Figure 5.

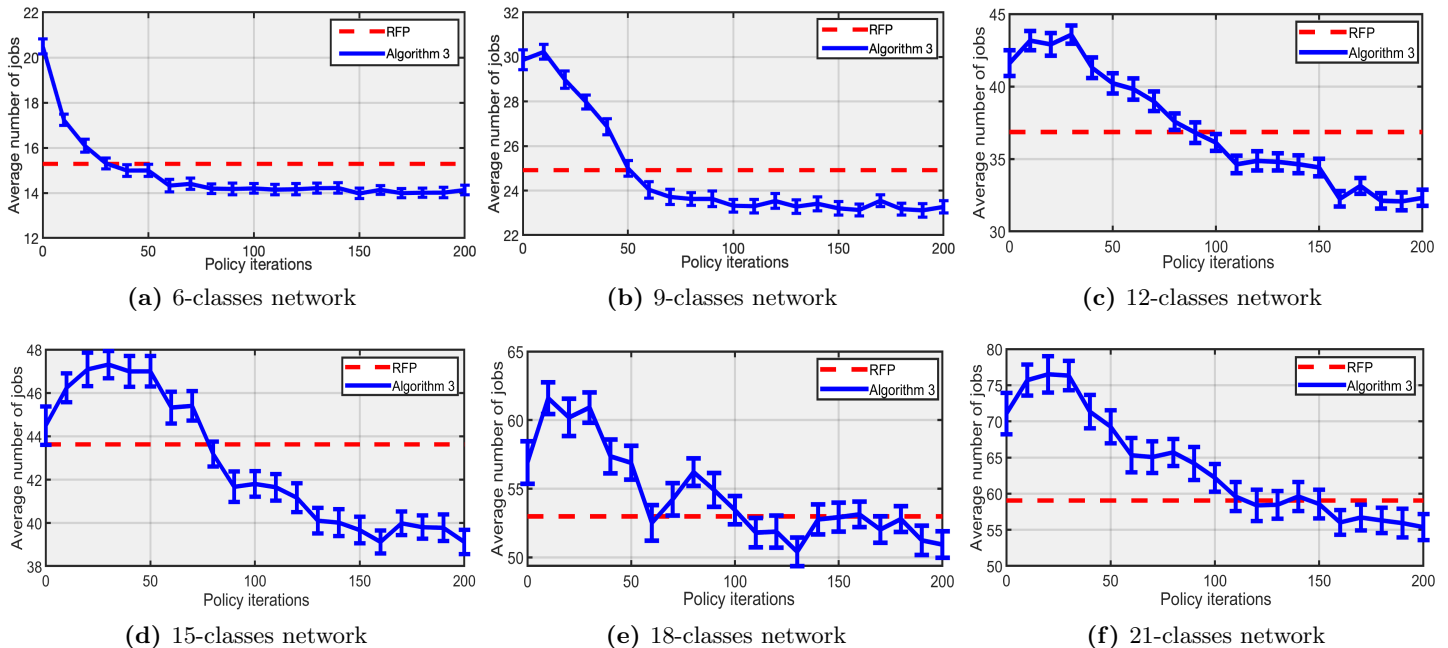


Figure 5: Performance of Algorithm 3 on six queueing networks. The solid blue lines show the performance of the PPO policies obtained at the end of every 10th iterations of Algorithm 3; the dashed red lines show the performance of the robust fluid policy (RFP).

In Section 4.3 we discussed the relationship between the GAE (4.26) and AMP (4.21) estimators. Figure 6 illustrates the benefits of using the AMP method in Algorithm 3 on the 6-classes network. The learning curve for the GAE estimator is obtained by replacing the value function estimation in line 6 of Algorithm 3 with the GAE estimator (4.26).

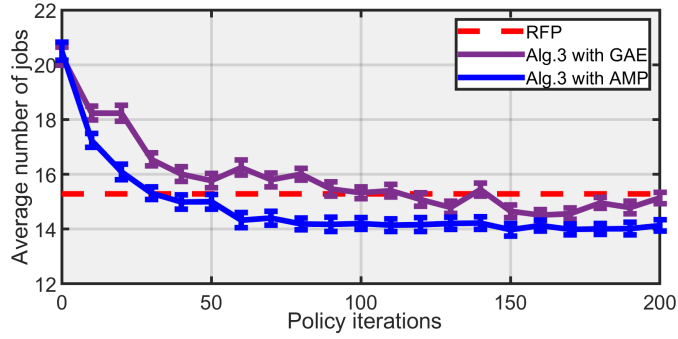


Figure 6: Learning curves from Algorithm 3 for the 6-class network. The solid blue and purple lines show the performance of the PPO policies obtained from Algorithm 3 in which the value function estimates are computed by the AMP method and by the GAE method, respectively; the dashed red line shows the performance of the robust fluid policy (RFP).

5.3 Parallel servers network

In this section we demonstrate that PPO Algorithm 3 is also effective for a stochastic processing network that is outside the model class of multiclass queueing networks. Figure 7 shows a processing network system with two independent Poisson input arrival flows, two servers, exponential service times, and linear holding costs. Known as the *N-model network*, it first appeared in [31].

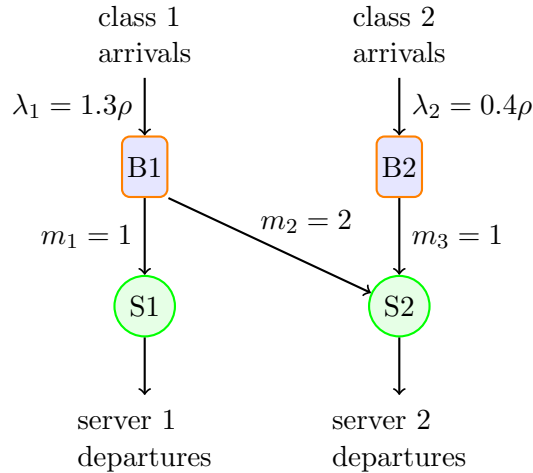


Figure 7: N-model network

Jobs of class i arrive according to a Poisson process at an average rate of λ_i such that $\lambda_1 = 1.3\rho$ and $\lambda_2 = 0.4\rho$ per unit time, where $\rho = 0.95$ is a parameter that specifies the traffic intensity. Each job requires a single service before it departs, and class 1 can be processed by either server 1 or server 2, whereas class 2 can be processed only by server 2. The jobs are processed by three different activities:

- activity 1 = processing of class 1 jobs by server 1,
- activity 2 = processing of class 1 jobs by server 2,
- activity 3 = processing of class 2 jobs by server 2.

We assume that the service at both servers is preemptive and work-conserving; specifically we assume that activity 2 occurs only if there is at least one class 1 job in the system.

The service times for activity i are exponentially distributed with mean m_i , where $m_1 = m_3 = 1$ and $m_2 = 2$. The holding costs are continuously incurred at a rate of h_j for each class j job that remains within the system, with the specific numerical values $h_1 = 3$ and $h_2 = 1$. We note that all model parameter values correspond to those in [31].

We define $x = (x_1, x_2) \in \mathcal{X}$ as a system state, where x_j is number of class j jobs in the system. We use uniformization to convert the continuous-time control problem to a discrete-time control problem. Under control $a = 1$ (class 1 has preemption high priority for server 2) the transition probabilities are given by

$$\begin{aligned} P((x_1 + 1, x_2)|(x_1, x_2)) &= \frac{\lambda_1}{\lambda_1 + \lambda_2 + \mu_1 + \mu_2 + \mu_3}, \\ P((x_1, x_2 + 1)|(x_1, x_2)) &= \frac{\lambda_2}{\lambda_1 + \lambda_2 + \mu_1 + \mu_2 + \mu_3}, \\ P((x_1 - 1, x_2)|(x_1, x_2), a = 1) &= \frac{\mu_1 \mathbb{I}_{\{x_1 > 0\}} + \mu_2 \mathbb{I}_{\{x_1 > 1\}}}{\lambda_1 + \lambda_2 + \mu_1 + \mu_2 + \mu_3}, \\ P((x_1, x_2 - 1)|(x_1, x_2), a = 1) &= \frac{\mu_3 \mathbb{I}_{\{x_2 > 0, x_1 \leq 1\}}}{\lambda_1 + \lambda_2 + \mu_1 + \mu_2 + \mu_3}, \\ P((x_1, x_2)|(x_1, x_2)) &= 1 - P((x_1 + 1, x_2)|(x_1, x_2)) - \\ &\quad - P((x_1, x_2 + 1)|(x_1, x_2)) - P((x_1 - 1, x_2)|(x_1, x_2)) - P((x_1, x_2)|(x_1, x_2), 1), \end{aligned}$$

where $\mu_i = 1/m_i$, $i = 1, 2, 3$.

Under control $a = 2$ (class 2 has high priority), the only changes of transition probabilities are

$$\begin{aligned} P((x_1 - 1, x_2)|(x_1, x_2), a = 2) &= \frac{\mu_1 \mathbb{I}_{\{x_1 > 0\}} + \mu_2 \mathbb{I}_{\{x_1 > 1, x_2 = 0\}}}{\lambda_1 + \lambda_2 + \mu_1 + \mu_2 + \mu_3}, \\ P((x_1, x_2 - 1)|(x_1, x_2), a = 2) &= \frac{\mu_3 \mathbb{I}_{\{x_2 > 0\}}}{\lambda_1 + \lambda_2 + \mu_1 + \mu_2 + \mu_3}. \end{aligned}$$

We define the cost-to-go function as $g(x) := h_1 x_1 + h_2 x_2 = 3x_1 + x_2$. The objective is to find policy $\pi_\theta, \theta \in \Theta$ that minimizes the long-run average holding costs

$$\lim_{N \rightarrow \infty} \frac{1}{N} \mathbb{E} \left[\sum_{k=0}^{N-1} g(x^{(k)}) \right],$$

where $x^{(k)}$ is the system state after k timesteps.

We use Algorithm 3 to find a near-optimal policy. Along with a learning curve from Algorithm 3, Figure 8 shows the performance the best threshold policy with $T = 11$ and the optimal policy. The threshold policy was proposed in [10]. Server 2 operating under the threshold policy gives priority to class 1 jobs, if the number of class 1 jobs in the system is larger than a fixed threshold T .

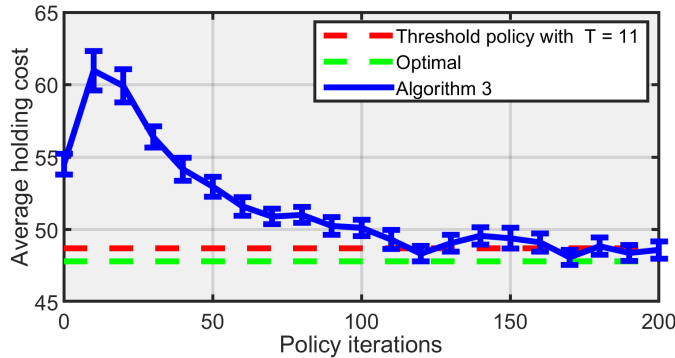


Figure 8: Learning curves from Algorithm 3 for the N-model network. The blue solid line shows the performance of PPO policies obtained from Algorithm 3; the dashed red line shows the performance of the threshold policy with $T = 11$; the dashed green line shows the performance of the optimal policy.

In Figure 9 we show the control of randomized PPO policies obtained after 1, 50, 100, 150, and 200 algorithm iterations. For each policy we depict the probability distribution over two possible actions for states $x \in \mathcal{X}$ such that $0 \leq x_j \leq 50$, $j = 1, 2$, and compare the PPO, optimal, and threshold policies.

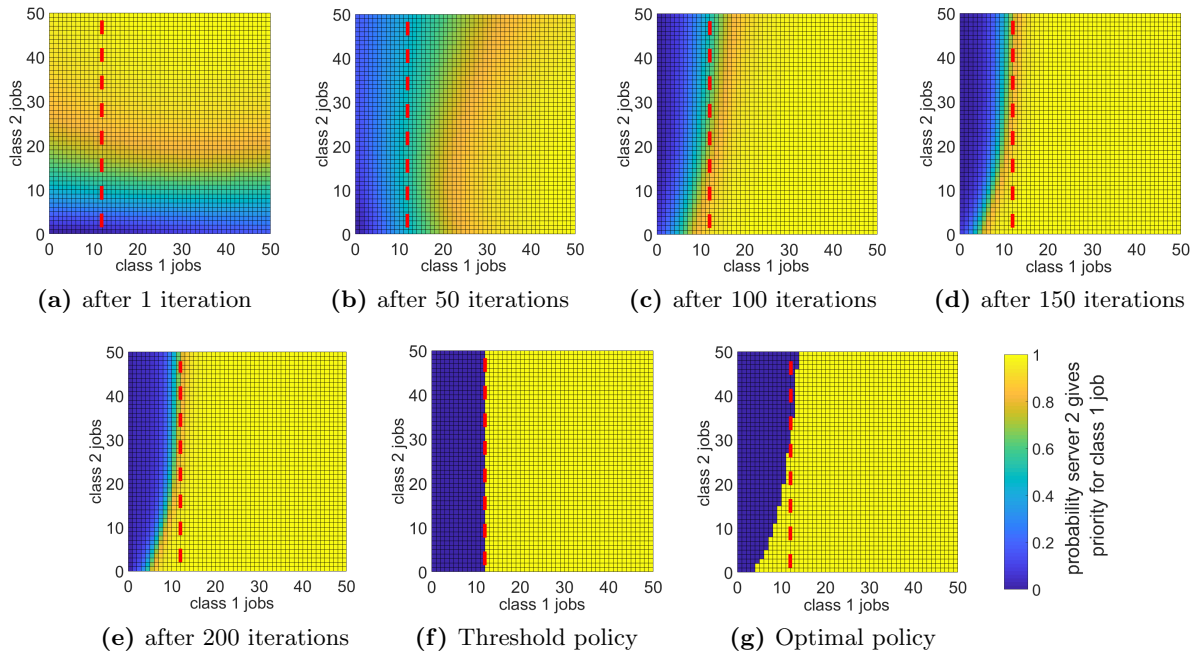


Figure 9: Evolution of the PPO policies over the learning process and comparing them with threshold and optimal policies. The probability that server 2 gives priority to class 1 jobs is shown by a color gradient for system states that have less than 50 jobs in each buffer: server 2 gives priority to class 1 jobs (yellow), server 2 gives priority to class 2 jobs (blue), and the dashed red lines represent the threshold policy with $T = 11$.

6 Conclusion

This paper proposed a method for optimizing the long-run average performance in queueing network control problems. It provided a theoretical justification for extending the PPO algorithm in [75] for Markov decision problems with infinite state space, unbounded costs, and the long-run average cost objective. Our idea of applying Lyapunov function approach has a potential to be adapted for other advanced policy gradient methods. We believe that theoretical analysis and performance comparison of policy gradient [56, 69], trust-region [73], proximal [75], soft actor-critic [28], deep Q-learning [62, 39], and other policy optimization algorithms can be of great benefit for the research community and deserve a separate study.

The success of the PPO algorithm implementation largely depends on the accuracy of Monte Carlo estimates of the relative value function in each policy iteration. Numerical experiments using sets of fixed hyperparameters showed that introducing an appropriate discount factor has the largest effect on the variance reduction of a value function estimator, even though the discount factor introduces biases, and that introducing a control variate by using the approximating martingale-process (AMP) further reduces the variance. Moreover, when system loads vary between light and moderate, regeneration estimators also reduce variances. The experiments also implied that AMP estimation, rather than GAE estimation, is preferable when the transition probabilities are known. Most of hyperparameters, including the discount factor and length of episodes, were chosen by experimental tuning rather than a theoretically justified scheme. It is desirable to investigate how to select the discount factor, length of episodes, and other hyperparameters based on queueing network load, size, topology.

Our numerical experiments demonstrated that Algorithm 2 applied for the criss-cross network control optimization can obtain policies with long-run average performance within 1% from the optimal. For large-size networks PPO Algorithm 3 produced effective control policies that either outperform or perform as well as the current alternatives. For an extended six-class queueing network, PPO policies outperform the robust fluid policies on average by 10%. The algorithm can be applied for a processing network control problem if the processing network admits a uniformization representation under any feasible control policy. A wide class of such processing networks described in [24]. As an example, we provide the numerical experiment for the N-model network. Although this paper considered only

queueing networks with preemptive service, the proposed algorithm can also be applied for queueing networks with non-preemptive service policies. Two modifications to the MDP formulation in Section 2 are required if a queueing network operates under non-preemptive service policies. First, a service status of each server should be included into the system state representation along with the jobcount vector. Second, at each decision time a set of feasible actions should be restricted based on each server status.

Several research questions should be pursued in future studies. First, future research could examine the necessity of \mathcal{V} -uniform ergodicity assumption in Theorem 1, and whether this assumption can be replaced by \mathcal{V} -ergodicity. Second, one of the key components of our PPO algorithm for MQNs is the proposed PR expert policy. Further research is needed to design an algorithm that does not require the knowledge of a stable expert policy. Third, our numerical experiments show that the variance reduction techniques are important for a good performance of the algorithm. Future investigations are desirable to develop more sample efficient simulation methods, potentially, incorporating problem structure knowledge.

Complexity of the queueing control optimization problems highly depends not only on the network topology, but on the traffic intensity. As the network traffic intensity increases the long-term effects of the actions become less predictable that presents a challenge for any reinforcement learning algorithm. We believe that multiclass queueing networks should serve as useful benchmarks for testing reinforcement learning methods.

Acknowledgment

This research was supported in part by National Science Foundation Grant CMMI-1537795.

Appendix

A Proofs of the theorems in Section 3

Proof of Lemma 3. We define vector $h := Z(g - (\mu^T g)e)$. Matrix Z has a finite \mathcal{V} -norm, therefore the inverse matrix of Z is unique and equal to $I - P + \Pi$. Then by definition vector h satisfies

$$(I - P + \Pi)h = g - (\mu^T g)e. \quad (\text{A.1})$$

Multiplying both sides of (A.1) by μ we get $\mu^T h = 0$ (and $\Pi h = 0$). Hence, vector h is a solution of the Poisson equation (3.3) such that $\mu^T h = 0$. It follows from Lemma 2 that $h = h^{(f)}$. \square

Proof of Lemma 4. We denote

$$U_{\theta,\eta} := (P_\theta - P_\eta)Z_\eta \quad (\text{A.2})$$

and define matrix $H_{\theta,\eta}$ as

$$H_{\theta,\eta} := \sum_{k=0}^{\infty} U_{\theta,\eta}^k. \quad (\text{A.3})$$

The convergence in the \mathcal{V} -weighted norm in definition (A.3) follows from assumption $\|U_{\theta,\eta}\|_{\mathcal{V}} < 1$.

The goal of this proof is to show that the Markov chain has a unique stationary distribution μ_θ such that

$$\mu_\theta^T = \mu_\eta^T H_{\theta,\eta}. \quad (\text{A.4})$$

We let $\nu^T := \mu_\eta^T H_{\theta,\eta}$. We use $e = (1, 1, \dots, 1, \dots)^T$ to denote the unit vector. First, we verify that $\nu^T e = \sum_{x \in \mathcal{X}} \nu(x) = 1$. We note that $Z_\eta e = e$. Then

$$\nu^T e = \mu_\eta^T H_{\theta,\eta} e = \mu_\eta^T \sum_{k=0}^{\infty} ((P_\theta - P_\eta)Z_\eta)^k e = \mu_\eta^T I e = 1.$$

Second, we verify that $\nu^T P_\theta = \nu^T$. We prove it by first assuming that

$$P_\theta - P_\eta + U_{\theta,\eta} P_\eta = U_{\theta,\eta} \quad (\text{A.5})$$

holds. Indeed,

$$\begin{aligned} \nu^T P_\theta &= \mu_\eta^T \sum_{k=0}^{\infty} U_{\theta,\eta}^k P_\theta \\ &= \mu_\eta^T \sum_{k=0}^{\infty} U_{\theta,\eta}^k P_\theta - \mu_\eta^T \sum_{k=0}^{\infty} U_{\theta,\eta}^k P_\eta + \mu_\eta^T \sum_{k=0}^{\infty} U_{\theta,\eta}^k P_\eta \\ &= \mu_\eta^T + \mu_\eta^T \sum_{k=0}^{\infty} U_{\theta,\eta}^k P_\theta - \mu_\eta^T \sum_{k=0}^{\infty} U_{\theta,\eta}^k P_\eta + \mu_\eta^T \sum_{k=0}^{\infty} U_{\theta,\eta}^{k+1} P_\eta \\ &= \mu_\eta^T + \mu_\eta^T \sum_{k=0}^{\infty} U_{\theta,\eta}^k (P_\theta - P_\eta + U_{\theta,\eta} P_\eta) \\ &= \mu_\eta^T + \mu_\eta^T \sum_{k=0}^{\infty} U_{\theta,\eta}^{k+1} \\ &= \mu_\eta^T \sum_{k=0}^{\infty} U_{\theta,\eta}^k \\ &= \nu^T. \end{aligned}$$

It remains to prove (A.5). Indeed,

$$\begin{aligned} P_\theta - P_\eta + U_{\theta,\eta} P_\eta &= P_\theta - P_\eta + (P_\theta - P_\eta) Z_\eta P_\eta \\ &= (P_\theta - P_\eta)(I + Z_\eta P_\eta) \\ &= (P_\theta - P_\eta)(I - \Pi_\eta + Z_\eta P_\eta) \\ &= (P_\theta - P_\eta)(I - Z_\eta \Pi_\eta + Z_\eta P_\eta) \\ &= (P_\theta - P_\eta) Z_\eta \\ &= U_{\theta,\eta}, \end{aligned}$$

where the second equality follows from

$$\left((P_\theta - P_\eta) Z_\eta \right) P_\eta = (P_\theta - P_\eta) (Z_\eta P_\eta),$$

which holds by [45, Corollary 1.9], the third equality holds due to $(P_\theta - P_\eta) \Pi_\eta = 0$, the fourth equality holds because $Z_\eta \Pi_\eta = \Pi_\eta$, and the fifth equality follows from $I = Z_\eta (I + \Pi_\eta - P_\eta) = Z_\eta + Z_\eta \Pi_\eta - Z_\eta P_\eta$.

The uniqueness of the stationary distribution follows from the fact that the Markov chain with transition matrix P_θ is assumed to be irreducible. \square

The following Lemma 9 will be used in the proofs of Theorem 1 and Lemma 5 below. We believe the claim of Lemma 9 should be a well-known mathematical fact, but we have not found its proof in any textbook. For completeness, we present it here.

Lemma 9. *Let $\mathcal{M}_{\mathcal{X},\mathcal{X}}$ be a set of all matrices on the countable space $\mathcal{X} \times \mathcal{X}$. The operator norm $\|\cdot\|_{\mathcal{V}}$ on $\mathcal{M}_{\mathcal{X} \times \mathcal{X}}$ is equivalent to the operator norm induced from vector norm $\|\cdot\|_{1,\mathcal{V}}$ and to the operator norm induced from vector norm $\|\cdot\|_{\infty,\mathcal{V}}$ in the following sense:*

$$\|T\|_{\mathcal{V}} = \sup_{\nu: \|\nu\|_{1,\mathcal{V}}=1} \|\nu T\|_{1,\mathcal{V}} = \sup_{h: \|h\|_{\infty,\mathcal{V}}=1} \|Th\|_{\infty,\mathcal{V}} \quad \text{for any } T \in \mathcal{M}_{\mathcal{X} \times \mathcal{X}},$$

where $\|\nu\|_{1,\mathcal{V}} = \sum_{x \in \mathcal{X}} |\nu(x)| \mathcal{V}(x)$, $\|\nu\|_{\infty,\mathcal{V}} = \sup_{x \in \mathcal{X}} \frac{|\nu(x)|}{\mathcal{V}(x)}$, $\|T\|_{\mathcal{V}} = \sup_{x \in \mathcal{X}} \frac{1}{\mathcal{V}(x)} \sum_{y \in \mathcal{X}} |T(x,y)| \mathcal{V}(y)$.

Furthermore, for any vectors ν_1, ν_2 on \mathcal{X} and matrices $T_1, T_2 \in \mathcal{M}_{\mathcal{X} \times \mathcal{X}}$ the following inequalities hold:

$$\|\nu_1^T T \nu_2\|_{\mathcal{V}} \leq \|\nu_1\|_{1,\mathcal{V}} \|T\|_{\mathcal{V}} \|\nu_2\|_{\infty,\mathcal{V}} \quad (\text{A.6})$$

and

$$\|T_1 T_2\|_{\mathcal{V}} \leq \|T_1\|_{\mathcal{V}} \|T_2\|_{\mathcal{V}}. \quad (\text{A.7})$$

Proof. First, we show that $\sup_{h: \|h\|_{1,\mathcal{V}}=1} \|Th\|_{1,\mathcal{V}} = \|T\|_{\mathcal{V}}$. On the one hand,

$$\begin{aligned} \sup_{\nu: \|\nu\|_{1,\mathcal{V}}=1} \|\nu T\|_{1,\mathcal{V}} &= \sup_{\nu: \mathcal{X} \rightarrow \mathbb{R}} \frac{1}{\|\nu\|_{1,\mathcal{V}}} \|\nu T\|_{1,\mathcal{V}} \\ &\geq \sup_{\nu \in \{e_x\}} \frac{1}{\|\nu\|_{1,\mathcal{V}}} \|\nu T\|_{1,\mathcal{V}} \\ &= \sup_{x \in \mathcal{X}} \frac{1}{\mathcal{V}(x)} \sum_{y \in X} \mathcal{V}(y) |T(x, y)| = \|T\|_{\mathcal{V}}, \end{aligned}$$

where in the second step we choose a set $\{e_x\}$ of unit vectors $e_x = (0, \dots, 0, 1, 0, \dots)$, where the x coordinate is 1 and the other coordinates are 0s.

On the other hand,

$$\begin{aligned} \|T\|_{\mathcal{V}} &= \sup_{x \in X} \sum_{y \in X} \frac{1}{\mathcal{V}(x)} |T(x, y)| \mathcal{V}(y) \sup_{\nu: \|\nu\|_{1,\mathcal{V}}=1} \sum_{x \in X} |\nu(x)| \mathcal{V}(x) \\ &\geq \sup_{\nu: \|\nu\|_{1,\mathcal{V}}=1} \sum_{y \in X} \sum_{x \in X} \frac{1}{\mathcal{V}(x)} |T(x, y)| \mathcal{V}(y) |\nu(x)| \mathcal{V}(x) \\ &= \sup_{\nu: \|\nu\|_{1,\mathcal{V}}=1} \sum_{y \in X} \sum_{x \in X} |T(x, y)| \nu(x) \mathcal{V}(y) \\ &= \sup_{\nu: \|\nu\|_{1,\mathcal{V}}=1} \|\nu T\|_{1,\mathcal{V}}. \end{aligned}$$

Similarly, we can show the equivalency of $\sup_{h: \|h\|_{\infty,\mathcal{V}}=1} \|Th\|_{\infty,\mathcal{V}}$ and $\|T\|_{\mathcal{V}}$ norms.

Inequalities (A.6) and (A.7) follow from the properties of a linear operator norm. \square

Proof of Theorem 1. We denote $U_{\theta,\eta} := (P_{\theta} - P_{\eta})Z_{\eta}$. Under assumption $\|U_{\theta,\eta}\|_{\mathcal{V}} = D_{\theta,\eta} < 1$ operator $H_{\theta,\eta} := \sum_{k=0}^{\infty} U_{\theta,\eta}^k$ is well-defined and

$$\|H_{\theta,\eta}\|_{\mathcal{V}} \leq \frac{1}{1 - D_{\theta,\eta}}. \quad (\text{A.8})$$

We represent the stationary distribution of the Markov chain with transition matrix P_{θ} as $\mu_{\theta}^T = \mu_{\eta}^T H_{\theta,\eta}$, see (A.4). We get

$$\|\mu_{\theta}\|_{1,\mathcal{V}} = \mu_{\theta}^T \mathcal{V} = \mu_{\eta}^T H_{\theta,\eta} \mathcal{V} \leq \|H_{\theta,\eta}\|_{\mathcal{V}} (\mu_{\eta}^T \mathcal{V}) < \infty, \quad (\text{A.9})$$

since $H_{\theta,\eta} \mathcal{V} \leq \|H_{\theta,\eta}\|_{\mathcal{V}} \mathcal{V}$ by definition of the \mathcal{V} -norm.

The long-run average costs difference is equal to

$$\begin{aligned} \mu_{\theta}^T g - \mu_{\eta}^T g &= \mu_{\theta}^T g + \mu_{\theta}^T ((P_{\theta} - I)h_{\eta}) - \mu_{\eta}^T g \\ &= \mu_{\theta}^T (g + P_{\theta} h_{\eta} - h_{\eta}) - \mu_{\eta}^T g \\ &= \mu_{\eta}^T (g - (\mu_{\eta}^T g)e + P_{\theta} h_{\eta} - h_{\eta}) + (\mu_{\theta}^T - \mu_{\eta}^T)(g + P_{\theta} h_{\eta} - h_{\eta}) \\ &= \mu_{\eta}^T (g - (\mu_{\eta}^T g)e + P_{\theta} h_{\eta} - h_{\eta}) + (\mu_{\theta}^T - \mu_{\eta}^T)(g - (\mu_{\eta}^T g)e + P_{\theta} h_{\eta} - h_{\eta}). \end{aligned}$$

Now we are ready to bound the last term:

$$\begin{aligned}
|(\mu_\theta^T - \mu_\eta^T)(g - (\mu_\eta^T g)e + P_\theta h_\eta - h_\eta)| &\leq \|\mu_\theta - \mu_\eta\|_{1,\mathcal{V}} \|g - (\mu_\eta^T g)e + P_\theta h_\eta - h_\eta\|_{\infty,\mathcal{V}} \\
&= \|\mu_\theta - \mu_\eta\|_{1,\mathcal{V}} \|(P_\theta - P_\eta)h_\eta\|_{\infty,\mathcal{V}} \\
&= \|\mu_\theta - \mu_\eta\|_{1,\mathcal{V}} \|(P_\theta - P_\eta)Z_\eta(g - (\mu_\eta^T g)e)\|_{\infty,\mathcal{V}} \\
&\leq \|\mu_\theta - \mu_\eta\|_{1,\mathcal{V}} \|(P_\theta - P_\eta)Z_\eta\|_{\mathcal{V}} \|g - (\mu_\eta^T g)e\|_{\infty,\mathcal{V}} \\
&= D_{\theta,\eta} \|\mu_\theta - \mu_\eta\|_{1,\mathcal{V}} \|g - (\mu_\eta^T g)e\|_{\infty,\mathcal{V}} \\
&= D_{\theta,\eta} \|\mu_\theta^T U_{\theta,\eta}\|_{1,\mathcal{V}} \|g - (\mu_\eta^T g)e\|_{\infty,\mathcal{V}}, \\
&\leq D_{\theta,\eta} \|\mu_\theta\|_{1,\mathcal{V}} \|U_{\theta,\eta}\|_{\mathcal{V}} \|g - (\mu_\eta^T g)e\|_{\infty,\mathcal{V}}, \\
&\leq D_{\theta,\eta}^2 \|\mu_\theta\|_{1,\mathcal{V}} \|g - (\mu_\eta^T g)e\|_{\infty,\mathcal{V}}, \\
&\leq D_{\theta,\eta}^2 \|H_{\theta,\eta}\|_{\mathcal{V}} \|g - (\mu_\eta^T g)e\|_{\infty,\mathcal{V}} (\mu_\eta^T \mathcal{V}), \\
&\leq \frac{D_{\theta,\eta}^2}{1 - D_{\theta,\eta}} \|g - (\mu_\eta^T g)e\|_{\infty,\mathcal{V}} (\mu_\eta^T \mathcal{V}),
\end{aligned}$$

where the first, second and third inequalities follow from Lemma 9, the second equality follows from Lemma 3, the last equality holds due to $\mu_\theta^T - \mu_\eta^T = \mu_\theta^T U_{\theta,\eta}$ from (A.4), the fourth inequality follows from (3.8), the fifth inequality follows from (A.9), and the last inequality holds due to (A.8). \square

Proof of Lemma 5.

$$\begin{aligned}
\|(P_\theta - P_\eta)Z_\eta\|_{\mathcal{V}} &\leq \|P_\theta - P_\eta\|_{\mathcal{V}} \|Z_\eta\|_{\mathcal{V}} \\
&= \|Z_\eta\|_{\mathcal{V}} \sup_{x \in \mathcal{X}} \frac{1}{\mathcal{V}(x)} \sum_{y \in \mathcal{X}} |P_\theta - P_\eta|_{x,y} \mathcal{V}(y) \\
&= \|Z_\eta\|_{\mathcal{V}} \sup_{x \in \mathcal{X}} \frac{1}{\mathcal{V}(x)} \sum_{y \in \mathcal{X}} \left| \sum_{a \in \mathcal{A}} P(y|x, a) \pi_\theta(a|x) - \sum_{a \in \mathcal{A}} P(y|x, a) \pi_\eta(a|x) \right| \mathcal{V}(y) \\
&\leq \|Z_\eta\|_{\mathcal{V}} \sup_{x \in \mathcal{X}} \frac{1}{\mathcal{V}(x)} \sum_{y \in \mathcal{X}} \sum_{a \in \mathcal{A}} P(y|x, a) |\pi_\theta(a|x) - \pi_\eta(a|x)| \mathcal{V}(y) \\
&= \|Z_\eta\|_{\mathcal{V}} \sup_{x \in \mathcal{X}} \sum_{a \in \mathcal{A}} |\pi_\theta(a|x) - \pi_\eta(a|x)| \frac{\sum_{y \in \mathcal{X}} P(y|x, a) \mathcal{V}(y)}{\mathcal{V}(x)} \\
&= \|Z_\eta\|_{\mathcal{V}} \sup_{x \in \mathcal{X}} \sum_{a \in \mathcal{A}} \left| \frac{\pi_\theta(a|x)}{\pi_\eta(a|x)} - 1 \right| G(x, a)
\end{aligned}$$

\square

B Proofs of the theorems in Section 4

We consider the Poisson equation for a Markov chain with the transition kernel P , stationary distribution μ , and cost function $g : \mathcal{X} \rightarrow \mathbb{R}$:

$$g(x) - \mu^T g + \sum_{y \in \mathcal{X}} P(y|x)h(y) - h(x) = 0, \text{ for each } x \in \mathcal{X},$$

which admits a solution

$$h^{(x^*)}(x) := \mathbb{E} \left[\sum_{k=0}^{\sigma(x^*)-1} (g(x^{(k)}) - \mu^T g) \mid x^{(0)} = x \right] \text{ for each } x \in \mathcal{X},$$

where $\sigma(x^*) = \min \{k > 0 \mid x^{(k)} = x^*\}$ is the first time when state x^* is visited.

Since regenerative cycles can be long in large-size systems, we propose to change the original dynamics and increase the probability of transition to the regenerative state x^* from each state $x \in \mathcal{X}$.

We let $P(y|x)$ be an original transition probability from state x to state y , for each $x, y \in \mathcal{X}$. We consider a new Markov reward process with cost function g and a modified transition kernel $\tilde{P}^{(\gamma)}$:

$$\begin{cases} \tilde{P}^{(\gamma)}(y|x) := \gamma P(y|x) & \text{for } y \neq x^*, \\ \tilde{P}^{(\gamma)}(x^*|x) := \gamma P(x^*|x) + (1 - \gamma), \end{cases} \quad (\text{B.1})$$

for each $x \in \mathcal{X}$.

We modified the transition kernel so that the probability of transition to the regenerative state x^* is at least $1 - \gamma$ from any state.

The Poisson equation for the modified problem is equal to:

$$g(x) - \tilde{\mu}^T g + \sum_{y \in \mathcal{X}} \tilde{P}^{(\gamma)}(y|x) \tilde{h}(y) - \tilde{h}(x) = 0, \text{ for each } x \in \mathcal{X}, \quad (\text{B.2})$$

where $\tilde{\mu}$ is the stationary distribution of the Markov chain $\tilde{P}^{(\gamma)}$.

Equation (B.2) admits a solution

$$\tilde{h}^{(x^*)}(x) := \mathbb{E} \left[\sum_{k=0}^{\tilde{\sigma}(x^*)-1} \left(g(x^{(k)}) - \tilde{\mu}^T g \right) \mid x^{(0)} = x \right] \text{ for each } x \in \mathcal{X}, \quad (\text{B.3})$$

where $x^{(k)}$ is the state of the Markov chain with transition matrix $\tilde{P}^{(\gamma)}$ after k timesteps, and $\tilde{\sigma}(x^*) = \min \{k > 0 \mid x^{(k)} = x^*\}$. According to the new dynamics the regeneration occurs more frequently and we can estimate solution (B.3) by using fewer replications of the regenerative simulation.

Lemma 10. Consider the Poisson equation for the Markov chain with the transition kernel $\tilde{P}^{(\gamma)}$ defined by (B.1), stationary distribution $\tilde{\mu}$, and cost function $g : \mathcal{X} \rightarrow \mathbb{R}$:

$$g(x) - \tilde{\mu}^T g + \sum_{y \in \mathcal{X}} \tilde{P}^{(\gamma)}(y|x) \tilde{h}(y) - \tilde{h}(x) = 0, \text{ for each } x \in \mathcal{X}. \quad (\text{B.4})$$

Equation (B.4) admits solutions:

$$J^{(\gamma)}(x) := \mathbb{E} \left[\sum_{k=0}^{\infty} \gamma^k \left(g(x^{(k)}) - \mu^T g \right) \mid x^{(0)} = x \right] \text{ for each } x \in \mathcal{X},$$

and

$$V^{(\gamma)}(x) := \mathbb{E} \left[\sum_{k=0}^{\sigma(x^*)-1} \gamma^k \left(g(x^{(k)}) - r(x^*) \right) \mid x^{(0)} = x \right] \text{ for each } x \in \mathcal{X},$$

where $x^{(k)}$ is the state of the Markov chain with transition matrix P after k timesteps.

Proof. We substitute the definition of $\tilde{P}^{(\gamma)}$ (B.1) and rewrite equation (B.4) as

$$g(x) - (\tilde{\mu}^T g - (1 - \gamma)\tilde{h}(x^*)) + \gamma \sum_{y \in \mathcal{X}} P(y|x) \tilde{h}(y) - \tilde{h}(x) = 0, \text{ for each } x \in \mathcal{X}. \quad (\text{B.5})$$

Equation (B.5) admits infinitely many solutions, but we specify a unique solution fixing $\tilde{h}(x^*)$. Next, we consider two options.

First, we let $\tilde{h}(x^*) = \frac{1}{1-\gamma}(\mu^T g - \tilde{\mu}^T g)$. Then the Poisson equation (B.5) becomes

$$g(x) - \mu^T g + \gamma \sum_{y \in \mathcal{X}} P(y|x) \tilde{h}(y) - \tilde{h}(x) = 0, \text{ for each } x \in \mathcal{X},$$

and admits solution

$$J^{(\gamma)}(x) := \mathbb{E} \left[\sum_{k=0}^{\infty} \gamma^k \left(g(x^{(k)}) - \mu^T g \right) \mid x^{(0)} = x \right] \text{ for each } x \in \mathcal{X}.$$

Second, we let $\tilde{h}(x^*) = 0$ in equation (B.5). We note that $\tilde{\mu}^T g = r(x^*)$, where $r(x^*) = (1 - \gamma)\mathbb{E}\left[\sum_{k=0}^{\infty} \gamma^k g(x^{(k)}) \mid x^{(0)} = x^*\right]$ is a present discounted value at x^* .

We get the Poisson equation (4.17)

$$g(x) - r(x^*) + \gamma \sum_{y \in \mathcal{X}} P(y|x)\tilde{h}(y) - \tilde{h}(x) = 0, \text{ for each } x \in \mathcal{X},$$

which admits solution (4.11)

$$V^{(\gamma)}(x) := \mathbb{E}\left[\sum_{k=0}^{\sigma(x^*)-1} \gamma^k \left(g(x^{(k)}) - r(x^*)\right) \mid x^{(0)} = x\right] \text{ for each } x \in \mathcal{X}.$$

Indeed,

$$\begin{aligned} V^{(\gamma)}(x) &= \mathbb{E}\left[\sum_{k=0}^{\infty} \gamma^k \left(g(x^{(k)}) - r(x^*)\right) \mid x^{(0)} = x\right] \\ &= \mathbb{E}\left[\sum_{k=0}^{\sigma(x^*)-1} \gamma^k \left(g(x^{(k)}) - r(x^*)\right) \mid x^{(0)} = x\right] + \mathbb{E}\left[\gamma^{\sigma(x^*)} \mathbb{E}\left[\sum_{k=0}^{\infty} \gamma^k \left(g(x^{(k)}) - r(x^*)\right) \mid x^{(0)} = x^*\right]\right] \\ &= \mathbb{E}\left[\sum_{k=0}^{\sigma(x^*)-1} \gamma^k \left(g(x^{(k)}) - r(x^*)\right) \mid x^{(0)} = x\right]. \end{aligned}$$

□

Proof of Lemma 7. By Lemma 10 function $V^{(\gamma)}$ is a solution of Poisson equation (B.2). We consider the discounted value function $J^{(\gamma)} = \mathbb{E}\left[\sum_{k=0}^{\infty} \gamma^k \left(g(x^{(k)}) - \mu^T g\right) \mid x^{(0)} = x\right]$ that is another solution.

Then, for an arbitrary $x \in \mathcal{X}$,

$$\left|V^{(\gamma)}(x) - h^{(x^*)}(x)\right| \leq \left|J^{(\gamma)}(x) - h^{(f)}(x)\right| + \left|V^{(\gamma)}(x) - h^{(x^*)}(x) - \left(J^{(\gamma)}(x) - h^{(f)}(x)\right)\right|, \quad (\text{B.6})$$

where $h^{(f)}$ is the fundamental solution of the Poisson equation (3.3).

First, we bound $|J^{(\gamma)}(x) - h^{(f)}(x)|$:

$$\begin{aligned} |J^{(\gamma)}(x) - h^{(f)}(x)| &\leq \sum_{t=0}^{\infty} |\gamma^t - 1| \left| \sum_{y \in \mathcal{X}} P^t(y|x)(g(y) - \mu^T g) \right| \\ &\leq R\mathcal{V}(x) \sum_{t=0}^{\infty} (1 - \gamma^t) r^t \\ &= R\mathcal{V}(x) r \frac{1 - \gamma}{(1 - r)(1 - \gamma r)}, \end{aligned}$$

where the second inequality follows from (3.2).

Since $V^{(\gamma)}$ and $J^{(\gamma)}$ are both solutions of the Poisson equation (B.2), therefore,

$$J^{(\gamma)}(x) - V^{(\gamma)}(x) = J^{(\gamma)}(x^*) - V^{(\gamma)}(x^*) = \frac{1}{1 - \gamma} (\mu^T g - r(x^*)) \text{ for each } x \in \mathcal{X}.$$

Similarly, $h^{(f)}(x) - h^{(x^*)}(x) = h^{(f)}(x^*)$ for each $x \in \mathcal{X}$.

Second, we bound the last term in inequality (B.6):

$$\begin{aligned}
& \left| V^{(\gamma)}(x) - h^{(x^*)}(x) - \left(J^{(\gamma)}(x) - h^{(f)}(x) \right) \right| \\
&= \left| h^{(f)}(x^*) - \frac{1}{1-\gamma}(r(x^*) - \mu^T g) \right| \\
&= \left| \sum_{t=0}^{\infty} \sum_{y \in \mathcal{X}} P^t(y|x^*)(g(y) - \mu^T g) - \sum_{t=0}^{\infty} \sum_{y \in \mathcal{X}} \gamma^t P^t(y|x^*)(g(y) - \mu^T g) \right| \\
&= \left| \sum_{t=0}^{\infty} \sum_{y \in \mathcal{X}} (1 - \gamma^t) P^t(y|x^*)(g(y) - \mu^T g) \right| \\
&\leq \sum_{t=0}^{\infty} |1 - \gamma^t| \left| \sum_{y \in \mathcal{X}} P^t(y|x^*)(g(y) - \mu^T g) \right| \\
&\leq R\mathcal{V}(x^*)r \frac{1 - \gamma}{(1-r)(1-\gamma r)},
\end{aligned}$$

where the last inequality holds due to (3.2). \square

Proof of Lemma 8. We denote $\bar{g}(x^{(k)}) := (g(x^{(k)}) - r(x^*))$. Following [61, Section 17.4.3], we can show that

$$\begin{aligned}
\text{Var}[\hat{V}^{(\gamma)}(x)] &= \mathbb{E} \left[\left(\sum_{k=0}^{\sigma(x^*)-1} \gamma^k \bar{g}(x^{(k)}) \right)^2 \mid x^{(0)} = x \right] - \left(V^{(\gamma)}(x) \right)^2 \\
&= \mathbb{E} \left[- \sum_{k=0}^{\sigma(x^*)-1} \gamma^{2k} \bar{g}^2(x^{(k)}) + 2 \sum_{k=0}^{\sigma(x^*)-1} \sum_{j=k}^{\sigma(x^*)-1} \gamma^{k+j} \bar{g}(x^{(k)}) \bar{g}(x^{(j)}) \mid x^{(0)} = x \right] - \left(V^{(\gamma)}(x) \right)^2 \\
&= \mathbb{E} \left[\sum_{k=0}^{\sigma(x^*)-1} \mathbb{E} \left[2 \sum_{j=k}^{\sigma(x^*)-1} \gamma^{k+j} \bar{g}(x^{(k)}) \bar{g}(x^{(j)}) - \gamma^{2k} \bar{g}^2(x^{(k)}) \mid \mathcal{F}_k \right] \mid x^{(0)} = x \right] - \left(V^{(\gamma)}(x) \right)^2 \\
&= \mathbb{E} \left[\sum_{k=0}^{\sigma(x^*)-1} 2\gamma^{2k} \bar{g}(x^{(k)}) \mathbb{E} \left[\sum_{j=k}^{\sigma(x^*)-1} \gamma^{j-k} \bar{g}(x^{(j)}) \mid \mathcal{F}_k \right] - \gamma^{2k} \bar{g}^2(x^{(k)}) \mid x^{(0)} = x \right] - \left(V^{(\gamma)}(x) \right)^2 \\
&= \mathbb{E} \left[\sum_{k=0}^{\sigma(x^*)-1} 2\gamma^{2k} \bar{g}(x^{(k)}) V^{(\gamma)}(x^{(k)}) - \gamma^{2k} \bar{g}^2(x^{(k)}) \mid x^{(0)} = x \right] - \left(V^{(\gamma)}(x) \right)^2,
\end{aligned}$$

where \mathcal{F}_k is a σ -algebra generated by x_0, x_1, \dots, x_k .

Hereafter, we denote $\sum_{y \in \mathcal{X}} P(y|x) V^{(\gamma)}(y)$ and $\sum_{y \in \mathcal{X}} P(y|x) (V^{(\gamma)}(y))^2$ as $PV^{(\gamma)}(x)$ and $P(V^{(\gamma)})^2(x)$, respectively, to improve readability. We use the Poisson equation (4.17) and replace $\bar{g}(x^{(k)})$ by $V^{(\gamma)}(x^{(k)}) - \gamma PV^{(\gamma)}(x^{(k)})$.

$$\begin{aligned}
& \mathbb{E} \left[\sum_{k=0}^{\sigma(x^*)-1} 2\gamma^{2k} \bar{g}(x^{(k)}) V^{(\gamma)}(x^{(k)}) - \gamma^{2k} \bar{g}^2(x^{(k)}) \mid x^{(0)} = x \right] - \left(V^{(\gamma)}(x) \right)^2 \\
&= \mathbb{E} \left[\sum_{k=0}^{\sigma(x^*)-1} \gamma^{2k} \left(2 \left(V^{(\gamma)}(x^{(k)}) - \gamma PV^{(\gamma)}(x^{(k)}) \right) V^{(\gamma)}(x_k) - \left(V^{(\gamma)}(x^{(k)}) - \gamma PV^{(\gamma)}(x^{(k)}) \right)^2 \right) \mid x^{(0)} = x \right] - \left(V^{(\gamma)}(x) \right)^2 \\
&= \mathbb{E} \left[\sum_{k=0}^{\sigma(x^*)-1} \gamma^{2k} \left(\left(V^{(\gamma)}(x^{(k)}) \right)^2 - \left(\gamma PV^{(\gamma)}(x^{(k)}) \right)^2 \right) \mid x^{(0)} = x \right] - \left(V^{(\gamma)}(x) \right)^2.
\end{aligned}$$

Next, we subtract the expectation of a martingale

$$\mathbb{E} \left[- \left(V^{(\gamma)}(x) \right)^2 + \gamma^{2\sigma(x^*)} \left(V^{(\gamma)}(x^{(\sigma(x^*)))} \right)^2 + \sum_{k=0}^{\sigma(x^*)-1} \gamma^{2k} \left(\left(V^{(\gamma)}(x^{(k)}) \right)^2 - \gamma^2 P \left(V^{(\gamma)} \right)^2 (x^{(k)}) \right) \mid x^{(0)} = x \right]$$

that is equal to zero by [37, Proposition 1]. Since $V^{(\gamma)}(x^{(\sigma(x^*))}) = 0$, we get

$$\begin{aligned} \text{Var}[\hat{V}^{(\gamma)}(x)] &= \mathbb{E} \left[\sum_{k=0}^{\sigma(x^*)-1} \gamma^{2k} \left(\gamma^2 P \left(V^{(\gamma)} \right)^2 (x^{(k)}) - \left(\gamma P V^{(\gamma)}(x^{(k)}) \right)^2 \right) \mid x^{(0)} = x \right] \\ &= \gamma^2 \mathbb{E} \left[\sum_{k=0}^{\sigma(x^*)-1} \gamma^{2k} \left(\text{Var} \left[V^{(\gamma)}(x^{(k+1)}) \mid x^{(k)} \right] \right) \mid x^{(0)} = x \right], \end{aligned}$$

where $\text{Var} \left[V^{(\gamma)}(x^{(k+1)}) \mid x^{(k)} \right] = \sum_{y \in \mathcal{X}} P(y|x^{(k)}) \left(V^{(\gamma)}(y) \right)^2 - \left(\sum_{y \in \mathcal{X}} P(y|x^{(k)}) V^{(\gamma)}(y) \right)^2$.

Next, we want to show that there exists constant $B_1 > 0$ such that for any $\gamma \in [0, 1]$

$$\left(V^{(\gamma)}(x) \right)^2 \leq B_1 \mathcal{V}(x) \quad \text{for each } x \in \mathcal{X}.$$

First, we recall that function $V^{(\gamma)}$ is a solution of Poisson equation (B.2) for the system with modified dynamics (B.1) and cost function g . Given that transition matrix P satisfies the drift condition (3.1), for the modified dynamics we have the following drift inequality

$$\sum_{y \in \mathcal{X}} \tilde{P}^{(\gamma)}(y|x) \mathcal{V}(y) \leq b \mathcal{V}(x) + (\mathcal{V}(x^*) + d) \mathbb{I}_{C \cup \{x: b \mathcal{V}(x) \leq \mathcal{V}(x^*)\}}(x) \quad \text{for each } x \in \mathcal{X},$$

for any $\gamma \in [0, 1]$. Indeed,

$$\begin{aligned} \sum_{y \in \mathcal{X}} \tilde{P}^{(\gamma)}(y|x) \mathcal{V}(y) &= \gamma \sum_{y \in \mathcal{X}} P(y|x) \mathcal{V}(y) + (1 - \gamma) \mathcal{V}(x^*) \\ &\leq \gamma b \mathcal{V}(x) + (1 - \gamma) \mathcal{V}(x^*) + d \mathbb{I}_C \\ &\leq b \mathcal{V}(x) + (\mathcal{V}(x^*) + d) \mathbb{I}_{C \cup \{x \in \mathcal{X}: b \mathcal{V}(x) \leq \mathcal{V}(x^*)\}}(x), \end{aligned}$$

where the first inequality follows from the drift condition (3.1), and the second inequality follows from the fact that $\gamma b \mathcal{V}(x) + (1 - \gamma) \mathcal{V}(x^*) \leq b \mathcal{V}(x)$ if $b \mathcal{V}(x) \geq \mathcal{V}(x^*)$, and $\gamma b \mathcal{V}(x) + (1 - \gamma) \mathcal{V}(x^*) \leq \mathcal{V}(x^*)$ otherwise.

Second, we use Jensen's inequality and get that function $\sqrt{\mathcal{V}}$ is also a Lyapunov function for the modified system:

$$\sum_{y \in \mathcal{X}} \tilde{P}^{(\gamma)}(y|x) \sqrt{\mathcal{V}(y)} \leq \sqrt{b \mathcal{V}(x)} + \sqrt{\mathcal{V}(x^*) + d} \mathbb{I}_{C \cup \{x \in \mathcal{X}: b \mathcal{V}(x) \leq \mathcal{V}(x^*)\}}(x) \quad \text{for each } x \in \mathcal{X}.$$

This drift inequality and the assumption that $|g(x)| \leq \sqrt{\mathcal{V}(x)}$ for each $x \in \mathcal{X}$ allow us to apply [61, Theorem 17.7.1], see also [61, equation (17.39)], and conclude that, for some $c_0 > 0$ independent of γ , Poisson equation (B.2) admits the fundamental solution $J^{(\gamma)} : \mathcal{X} \rightarrow \mathbb{R}$ such that

$$|J^{(\gamma)}(x)| \leq c_0 (\sqrt{\mathcal{V}(x)} + 1), \quad \text{for each } x \in \mathcal{X}.$$

Function $V^{(\gamma)}$ is another solution of Poisson equation (B.2), such that $J^{(\gamma)}(x) = V^{(\gamma)}(x) + J^{(\gamma)}(x^*)$, for each $x \in \mathcal{X}$, because $V^{(\gamma)}(x^*) = 0$. Since $\mathcal{V} \geq 1$, there exists constant $B_1 > 0$ such that

$$|V^{(\gamma)}(x)| \leq |J^{(\gamma)}(x)| + |J^{(\gamma)}(x^*)| \leq c_0 (\sqrt{\mathcal{V}(x)} + 1) + c_0 (\sqrt{\mathcal{V}(x^*)} + 1) \leq \sqrt{B_1 \mathcal{V}(x)}, \quad \text{for each } x \in \mathcal{X}.$$

We have proved that, for some constant $B_1 > 0$,

$$\left(V^{(\gamma)}(x) \right)^2 \leq B_1 \mathcal{V}(x) \quad \text{for each } x \in \mathcal{X},$$

for any $\gamma \in [0, 1]$.

We let $G^{(\gamma)}(x) := \text{Var} [V^{(\gamma)}(x^{(1)}) \mid x^{(0)} = x]$. Then there exists a positive constant B such that

$$G^{(\gamma)}(x) \leq \sum_{y \in \mathcal{X}} P(y|x) \left(V^{(\gamma)}(y) \right)^2 \leq B_1 P\mathcal{V}(x) \leq B\mathcal{V}(x), \quad (\text{B.7})$$

where the last inequality follows from the drift condition (3.1). By [61, Theorem 15.0.1] we have that there exist constants $R > 0$ and $r \in (0, 1)$ such that

$$\left| P^k G^{(\gamma)}(x) - \beta^{(\gamma)} \right| \leq R\mathcal{V}(x)r^k, \quad (\text{B.8})$$

where $\beta^{(\gamma)} := \sum_{x \in \mathcal{X}} \mu(x) G^{(\gamma)}(x)$ is a discounted asymptotic variance.

Then

$$\begin{aligned} \text{Var}[\hat{V}^{(\gamma)}(x)] &= \gamma^2 \mathbb{E} \left[\sum_{k=0}^{\sigma(x^*)-1} \gamma^{2k} \left(\text{Var} [V^{(\gamma)}(x^{(k+1)}) \mid x^{(k)}] \right) \mid x^{(0)} = x \right] \\ &\leq \gamma^2 \sum_{k=0}^{\infty} \gamma^{2k} \mathbb{E}[G^{(\gamma)}(x_k) \mid x_0 = x] \\ &\leq \gamma^2 \sum_{k=0}^{\infty} \gamma^{2k} \left(R\mathcal{V}(x)r^k + \beta^{(\gamma)} \right) \\ &= \gamma^2 \left(R\mathcal{V}(x) \frac{1}{1-\gamma^2 r} + \beta^{(\gamma)} \frac{1}{1-\gamma^2} \right) \\ &\leq \gamma^2 \left(R\mathcal{V}(x) \frac{1}{1-\gamma^2 r} + (\mu^T \mathcal{V}) B \frac{1}{1-\gamma^2} \right), \end{aligned}$$

where the second inequality follows from (B.8) and the last inequality follows from (B.7). \square

C Maximal stability of the proportionally randomized policy

We assert that a discrete-time MDP obtained by uniformization of the multiclass queueing network SMDP model is stable under the proportionally randomized (PR) policy if the load conditions (2.9) are satisfied. We illustrate the proof for the criss-cross queueing network. We let $x \in \mathbb{Z}_+^3$ be a state for the discrete-time MDP. The proportionally randomized policy π is given by

$$\pi(x) = \begin{cases} \left(\frac{x_1}{x_1+x_3}, 1, \frac{x_3}{x_1+x_3} \right) & \text{if } x_2 \geq 1 \text{ and } x_1 + x_3 \geq 1, \\ \left(\frac{x_1}{x_1+x_3}, 0, \frac{x_3}{x_1+x_3} \right) & \text{if } x_2 = 0 \text{ and } x_1 + x_3 \geq 1, \\ (0, 1, 0) & \text{if } x_2 \geq 1 \text{ and } x_1 + x_3 = 0, \\ (0, 0, 0) & \text{if } x_2 = 0 \text{ and } x_1 + x_3 = 0. \end{cases}$$

Recall the transition probabilities \tilde{P} defined by (2.5). The discrete-time MDP operating under policy π is a DTMC. Now we can specify its transition matrix. For $x \in \mathbb{Z}_+^3$ with $x_1 \geq 1$, $x_3 \geq 1$, and $x_2 \geq 1$,

$$P(y|x) = \pi_1(x) \tilde{P}(y|x, (1, 2)) + \pi_3(x) \tilde{P}(y|x, (3, 2)) \quad \text{for each } y \in \mathbb{Z}_+^3.$$

For $x \in \mathbb{Z}_+^3$ on the boundary with $x_1 \geq 1$, $x_3 \geq 1$, and $x_2 = 0$,

$$P(y|x) = \pi_1(x) \tilde{P}(y|x, (1, 0)) + \pi_3(x) \tilde{P}(y|x, (3, 0)) \quad \text{for each } y \in \mathbb{Z}_+^3.$$

For $x \in \mathbb{Z}_+^3$ on the boundary with $x_1 = 0$, $x_3 \geq 1$, and $x_2 \geq 1$,

$$P(y|x) = \tilde{P}(y|x, (3, 2)) \quad \text{for each } y \in \mathbb{Z}_+^3.$$

Similarly, we write the transition probabilities for other boundary cases. One can verify that

$$P((x_1 + 1, x_2, x_3)|x) = \frac{\lambda_1}{B}, \quad P((x_1, x_2, x_3 + 1)|x) = \frac{\lambda_3}{B}, \quad (\text{C.1})$$

$$P((x_1 - 1, x_2 + 1, x_3)|x) = \frac{\mu_1}{B} \frac{x_1}{x_1 + x_3} \quad \text{if } x_2 \geq 1, \quad (\text{C.2})$$

$$P((x_1, x_2, x_3 - 1)|x) = \frac{\mu_3}{B} \frac{x_3}{x_1 + x_3} \quad \text{if } x_3 \geq 1, \quad (\text{C.3})$$

$$P((x_1, x_2 - 1, x_3)|x) = \frac{\mu_2}{B} \quad \text{if } x_2 \geq 1, \quad (\text{C.4})$$

$$P(x|x) = 1 - \sum_{y \neq x} P(y|x), \quad (\text{C.5})$$

where $B = \lambda_1 + \lambda_3 + \mu_1 + \mu_2 + \mu_3$. This transition matrix P is irreducible. Now we consider the continuous-time criss-cross network operating under the head-of-line proportional-processor-sharing (HLPPS) policy defined in [17]. Under the HLPPS policy, the jobcount process $\{Z(t), t \geq 0\}$ is a CTMC. Under the load condition (2.1), [17] proves that the CTMC is positive recurrent. One can verify that the transition probabilities in (C.1)-(C.5) are identical to the ones for a uniformized DTMC of this CTMC. Therefore, the DTMC corresponding to the transition probabilities (C.1)-(C.5) is positive recurrent, and proves the stability of the discrete-time MDP operating under the proportionally randomized policy.

D Additional experimental results

In Remark 5 we discussed two possible biased estimators of the solution to the Poisson equation. In this section we compare the performance of the PPO algorithm with these two estimators. We consider two versions of line 7 in Algorithm 3: Version 1 uses the regenerative discounted value function (VF) estimator (4.21), and Version 2 uses the discounted value function estimator (4.24). We apply two versions of the PPO algorithm for the criss-cross network operating under the balanced medium (B.M.) load regime. The queueing network parameter setting is identical to the one detailed in Section 5.1, except that the quadratic cost function $g(x) = x_1^2 + x_2^2 + x_3^2$ replaces the linear cost function that is used to minimize the long-run average cost, where x_i is a number of jobs in buffer i , $i = 1, 2, 3$.

We use Xavier initialization to initialize the policy NN parameters θ_0 . We take the empty system state $x^* = (0, 0, 0)$ as a regeneration state. Each episode in each iteration starts at the regenerative state and runs for 6,000 timesteps. We compute the one-replication estimates of a value function (either regenerative discounted VF or discounted VF) for the first $N = 5,000$ steps at each episode. In this experiment we simulated $Q = 20$ episodes in parallel. The values of the remaining hyperparameters (not mentioned yet) are the same as in Table 6.

In Figure 10 we compare the learning curves of PPO algorithm 3 empirically to demonstrate the benefits of using the regenerative discounted VF estimator over the discounted VF estimator when the system regeneration occurs frequently.

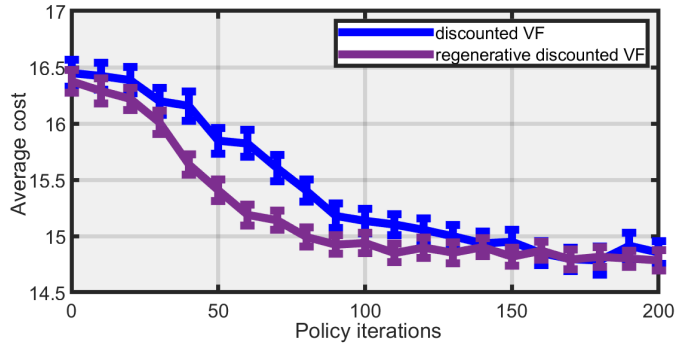


Figure 10: Learning curves from Algorithm 3 for the criss-cross network with the B.M. load and quadratic cost function. The solid purple and blue lines show the performance of the PPO policies obtained from Algorithm 3 in which the solutions to the Poisson equations are estimated by the discounted VF estimator and by the regenerative discounted VF estimator, respectively.

E Neural network structure

In the experiments we parameterized the RL policy with a neural network. Here, we use θ to denote the vector of weights and biases of the neural network. For a fixed parameter θ , the neural network outputs deterministically distribution $\pi_\theta(\cdot|x)$ over the action space for each state $x \in \mathcal{X}$. Therefore, the resulting policy π_θ is a randomized policy as explained in Section 2.

To represent the policy we use a fully connected feed-forward neural network with one input layer, three hidden layers with tanh activation functions, and one output layer. The input layer has J units, one for each job class, the first hidden layer has $10 \times J$ units, the third hidden layer has $10 \times L$, where L is number of stations in the queueing system. The number of units in the second hidden layer is a geometric mean of units in the first and third hidden layers (i.e. $10 \times \sqrt{LJ}$).

We use $z_j^{(k)}$ to denote the variable in the j th unit of hidden layer k , $k = 1, 2, 3$. Thus, our feed-forward neural network has the following representations:

$$\begin{aligned} z_j^{(1)} &= h\left(\sum_{i=1}^J A_{ji}^{(1)} x_i + b_j^{(1)}\right), \quad j = 1, \dots, 10J, \\ z_j^{(2)} &= h\left(\sum_{i=1}^{10J} A_{ji}^{(2)} z_i^{(1)} + b_j^{(2)}\right), \quad j = 1, \dots, 10\sqrt{LJ}, \\ z_j^{(3)} &= h\left(\sum_{i=1}^{10\sqrt{LJ}} A_{ji}^{(3)} z_i^{(2)} + b_j^{(3)}\right), \quad j = 1, \dots, 10\sqrt{L}, \end{aligned}$$

where $h: \mathbb{R} \rightarrow \mathbb{R}$ is the activation function given by $h(y) = \tanh(y)$ for each $y \in \mathbb{R}$.

We denote $p = (p_j)$ as the output vector, which is given by

$$p_j = \sum_{i=1}^{10\sqrt{L}} A_{ji}^{(4)} z_i^{(3)} + b_j^{(4)}, \quad j \in \mathcal{J},$$

and normalize output vector p via a *softmax function* into L probability distributions as:

$$\pi_\theta(j|x) = \frac{\exp(p_j)}{\sum_{i \in \mathcal{L}(\ell)} \exp(p_i)} \quad \text{for each } j \in \mathcal{B}(\ell), \ell \in \mathcal{L}, \quad (\text{E.1})$$

where the sets \mathcal{J} , \mathcal{L} , and $\mathcal{B}(\ell)$ are defined in Section 2.

The neural network parameter θ is the vector of weights A 's and biases b 's

$$\theta = \left(A^{(1)}, b^{(1)}, A^{(2)}, b^{(2)}, A^{(3)}, b^{(3)}, A^{(4)}, b^{(4)}\right),$$

which has dimension

$$K = (J \times 10J + 10J) + (10J \times 10\sqrt{LJ} + 10\sqrt{LJ}) + (10\sqrt{LJ} \times 10L + 10L) + (10L \times J + J).$$

For example, when $J = 21$ and $L = 7$, this dimension is approximately equal to 30203.

To represent the value function we use a neural network whose architecture is almost identical to the policy neural network except that the third hidden layer has 10 units. The number of units in the second hidden layer is $10 \times \sqrt{J}$. The output layer contains one unit with a linear activation function, which means that

$$V(x) = \sum_{i=1}^{10} A_i^{(4)} z_i^{(3)} + b^{(4)}.$$

For the N-model processing network in Section 5.3 the structure of policy and value NNs is the same as for the MQNs described above, except for the meaning of set $\mathcal{B}(\ell)$ in (E.1). We consider station $\ell \in \mathcal{L}$ of a processing network. The set $\mathcal{B}(\ell)$ includes a job class if and only if there is an activity such that station ℓ can process jobs from this class.

F Implementation details and experiment parameters

We use Tensorflow v1.13.1 [1] to build a training routine of the neural networks and Ray package v0.6.6 [64] to maintain parallel simulation of the actors. We run all experiments on a 2.7 GHz 96-core processor with 1510 GB of RAM.

We optimize the value and policy functions to minimize the corresponding loss functions (4.4), (4.7) by the Adaptive Moment Estimation (Adam) method [46]. The Adam method is an algorithm for mini-batch gradient-based optimization. We assume that N datapoints have been generated $D^{(1:N)} = \left\{ (x^{(j)}, a^{(j)}, \hat{A}_j) \right\}_{j=1}^N$ to update the policy NN or $D^{(1:N)} = \left\{ (x^{(j)}, \hat{V}_j) \right\}_{j=1}^N$ to update the value NN. The Adam algorithm runs for E epochs. The number of epochs is the number of complete passes through the entire dataset. In the beginning of a new epoch e the entire dataset is randomly reshuffled and divided into batches with size m . Then each batch (indexed by n) is passed to the learning algorithm and the parameters of the neural networks $\theta = (\theta^1, \dots, \theta^i, \dots, \theta^K)$ are updated at the end of every such step according to

$$\theta_{n+1}^i = \theta_n^i - \varsigma \frac{1}{\sqrt{\hat{H}_n^i + \varrho}} \hat{G}_n^i,$$

where ς is a learning rate, \hat{G}_n and \hat{H}_n are moving average estimates of the first and second moments of the gradient, respectively, and $\varrho \ll 1$ is a constant.

We use the batches to compute the gradient of a loss function $\hat{L}(\theta, D)$, such as for (4.7):

$$g_n = \frac{1}{m} \nabla_{\theta} L \left(\theta, D_e^{(nm:nm+m)} \right), \quad (\text{F.1})$$

where $D_e^{(nm:nm+m)}$ denotes the data segment in the n th batch of size m at epoch e .

The moving averages G_0 and H_0 are initialized as vectors of zeros at the first epoch. Then the Adam method updates the moving average estimates and includes bias corrections to account for their initialization at the origin:

$$\begin{cases} G_n = \beta_1 G_{n-1} + (1 - \beta_1) g_{n-1}, \\ \hat{G}_n = \frac{G_n}{1 - \beta_1^n}, \end{cases}$$

where $\beta_1 > 0$, with β_1^n denoting β_1 to the power n .

Similarly, we compute the second moments by

$$\begin{cases} H_n = \beta_2 H_{n-1} + (1 - \beta_2) g_{n-1}^2, \\ \hat{H}_n = \frac{H_n}{1 - \beta_2^n}, \end{cases}$$

where g_n^2 means the elementwise square, $\beta_2 > 0$ with β_2^n denoting β_2 to the power n .

Each subsequent epoch continues the count over n and keeps updating the moving average estimates G_n, H_n starting from their final values of the latest epoch.

Table 5 and Table 6 list the PPO hyperparameters we choose for the experiments in Section 5. Table 7 reports the estimates of the running time of Algorithm 3.

Parameter	Value
Clipping parameter (ϵ)	$0.2 \times \max[\alpha, 0.01]$
No. of regenerative cycles per actor (N)	5,000
No. of actors (Q)	50
Adam parameters for policy NN	$\beta_1 = 0.9, \beta_2 = 0.999, \varrho = 10^{-8}, \varsigma = 5 \cdot 10^{-4} \times \max[\alpha, 0.05]$
Adam parameters for value NN	$\beta_1 = 0.9, \beta_2 = 0.999, \varrho = 10^{-8}, \varsigma = 2.5 \cdot 10^{-4}$
No. of epochs (E)	3
Minibatch size in Adam method (m)	2048

Table 5: PPO hyperparameters used in Algorithms 1 and 2 for the experiments in Section 5.1. Parameter α decreases linearly from 1 to 0 over the course of learning: $\alpha = (I - i)/I$ on the i th policy iteration, $i = 0, 1, \dots, I - 1$.

Parameter	Value
Clipping parameter (ϵ)	$0.2 \times \max[\alpha, 0.01]$
Horizon (N)	50,000
No. of actors (Q)	50
Adam parameters for policy NN	$\beta_1 = 0.9, \beta_2 = 0.999, \rho = 10^{-8}, \varsigma = 5 \cdot 10^{-4} \times \max[\alpha, 0.05]$
Adam parameters for policy NN	$\beta_1 = 0.9, \beta_2 = 0.999, \rho = 10^{-8}, \varsigma = 2.5 \cdot 10^{-4}$
Discount factor (β)	0.998
GAE parameter (λ)	0.99
No. of epochs (E)	3
Minibatch size in Adam method (m)	2048

Table 6: PPO hyperparameters used in Algorithm 3 for the experiments in Sections 5.2 and 5.3. Parameter α decreases linearly from 1 to 0 over the course of learning: $\alpha = (I - i)/I$ on the i th policy iteration, $i = 0, 1, \dots, I - 1$.

Num. of classes $3L$	Time (minutes)
6	0.50
9	0.73
12	1.01
15	2.12
18	4.31
21	7.61

Table 7: Running time of *one policy iteration* of Algorithm 3 for the extended six-class network in Figure 4.

In the Algorithm 3 we use finite length episodes to estimate the expectation of the loss function in line 10. For each episode we need to specify an initial state. We propose sampling the initial states from the set of states generated during previous policy iterations. We consider the i th policy iteration of the algorithm. We need to choose initial states to simulate policy π_i . Since policy π_{i-1} has been simulated in the $(i - 1)$ th iteration of the algorithm, we can sample Q states uniformly at random from the episodes generated under policy π_{i-1} and save them in memory. Then we use them as initial states for Q episodes under π_i policy. For policy π_0 all Q episodes start from state $x = (0, \dots, 0)$.

References

- [1] M. Abadi, P. Barham, J. Chen, Z. Chen, A. Davis, J. Dean, M. Devin, S. Ghemawat, G. Irving, M. Isard, M. Kudlur, J. Levenberg, R. Monga, S. Moore, D. G. Murray, B. Steiner, P. Tucker, V. Vasudevan, P. Warden, M. Wicke, Y. Yu, and X. Zheng. Tensorflow: A system for large-scale machine learning. In *12th USENIX Symposium on Operating Systems Design and Implementation (OSDI 16)*, pages 265–283. USENIX Association, 2016.
- [2] Yasin Abbasi-Yadkori, Peter Bartlett, and Alan Malek. Linear programming for large-scale markov decision problems. In *Proceeding ICML’14*, volume 32, pages 496–504, 2014.
- [3] Ilge Akkaya, Marcin Andrychowicz, Maciek Chociej, and et.al. Solving rubik’s cube with a robot hand. 2019. URL: <https://arxiv.org/abs/1910.07113>.
- [4] Sigrún Andradóttir, Daniel P. Heyman, and Teunis J. Ott. Variance reduction through smoothing and control variates for Markov chain simulations. *ACM Transactions on Modeling and Computer Simulation (TOMACS)*, 3(3):167–189, 1993.
- [5] Søren Asmussen. *Applied Probability and Queues*. Springer, New York, 2003.
- [6] Baris Ata and Sunil Kumar. Heavy traffic analysis of open processing networks with complete resource pooling: asymptotic optimality of discrete review policies. *Annals of Applied Probability*, 15:331–391, 2005.

- [7] Florin Avram, Dimitris Bertsimas, and Michael Ricard. Fluid models of sequencing problems in open queueing networks: an optimal control approach. In F. Kelly and R. J. Williams, editors, *Stochastic Networks*, volume 71, page 237. Springer, New York, 1995.
- [8] Nicole Bäuerle. Asymptotic optimality of tracking policies in stochastic networks. *The Annals of Applied Probability*, 10(4):1065–1083, 2001.
- [9] Jonathan Baxter and Peter L. Bartlett. Infinite-horizon policy-gradient estimation. *Journal of Artificial Intelligence Research*, 15(1):319–350, 2001.
- [10] S. L. Bell and R. J. Williams. Dynamic scheduling of a system with two parallel servers in heavy traffic with resource pooling: asymptotic optimality of a threshold policy. *The Annals of Applied Probability*, 11(3):608–649, 2001.
- [11] Marc G. Bellemare, Yavar Naddaf, Joel Veness, and Michael Bowling. The arcade learning environment: an evaluation platform for general agents. *Journal of Artificial Intelligence Research*, 47(1):253–279, 2013.
- [12] D. Bertsimas, I. C. Paschalidis, and J. Tsitsiklis. Optimization of multiclass queueing networks: Polyhedral and nonlinear characterizations of achievable performance. *The Annals of Applied Probability*, 4:43–75, 1994.
- [13] Dimitris Bertsimas, David Gamarnik, and Alexander Anatoliy Rikun. Performance analysis of queueing networks via robust optimization. *Operations Research*, 59(2):455–466, 2011.
- [14] Dimitris Bertsimas, Ebrahim Nasrabadi, and Ioannis Ch. Paschalidis. Robust fluid processing networks. *IEEE Transactions on Automatic Control*, 60(3):715–728, 2015.
- [15] Frederick J. Beutler and Keith W. Ross. Uniformization for semi-Markov decision processes under stationary policies. *Journal of Applied Probability*, 24(3):644–656, 1987.
- [16] Shalabh Bhatnagar and K. Lakshmanan. An online actor-critic algorithm with function approximation for constrained Markov decision processes. *Journal of Optimization Theory and Applications*, 153(3):688–708, 2012.
- [17] Maury Bramson. Convergence to equilibria for fluid models of head-of-the-line proportional processor sharing queueing networks. *Queueing Systems*, 23(1-4):1–26, 1996.
- [18] Maury Bramson. State space collapse with application to heavy traffic limits for multiclass queueing networks. *Queueing Systems. Theory and Applications*, 30:89–140, 1998.
- [19] Hong Chen and David Yao. Dynamic scheduling of a multiclass fluid network. *Operations Research*, 41:1104–1115, 1993.
- [20] Rong-Rong Chen and Sean Meyn. Value iteration and optimization of multiclass queueing networks. *Queueing Systems*, 32:65–97, 1999.
- [21] W. Chen, D. Huang, A. A. Kulkarni, J. Unnikrishnan, Q. Zhu, P. Mehta, S. Meyn, and A. Wierman. Approximate dynamic programming using fluid and diffusion approximations with applications to power management. In *Proceedings of the 48th IEEE Conference on Decision and Control (CDC) held jointly with 2009 28th Chinese Control Conference*, pages 3575–3580, Dec 2009. doi:10.1109/CDC.2009.5399685.
- [22] William L. Cooper, Shane G. Henderson, and Mark E. Lewis. Convergence of simulation-based policy iteration. *Probability in the Engineering and Informational Sciences*, 17(2):213–234, 2003.
- [23] J. G. Dai. A fluid limit model criterion for instability of multiclass queueing networks. *The Annals of Applied Probability*, 6(3):751–757, 1996.
- [24] J. G. Dai and J. Michael Harrison. *Processing Networks: Fluid Models and Stability*. Cambridge University Press, Cambridge, UK, 2020. URL: <http://spnbook.org>.

- [25] J. G. Dai and Pengyi Shi. Inpatient overflow: An approximate dynamic programming approach. *Manufacturing & Service Operations Management*, 21(4):894–911, 2019.
- [26] D. P. de Farias and B. Van Roy. The linear programming approach to approximate dynamic programming. *Operations Research*, 51(6):850–865, 2003.
- [27] Xavier Glorot and Yoshua Bengio. Understanding the difficulty of training deep feedforward neural networks. In *Proceedings of the Thirteenth International Conference on Artificial Intelligence and Statistics*, pages 249–256, 2010.
- [28] Tuomas Haarnoja, Aurick Zhou, Pieter Abbeel, and Sergey Levine. Soft actor-critic: Off-policy maximum entropy deep reinforcement learning with a stochastic actor. *ICML 2018*, 5:2976–2989, 2018.
- [29] J. Michael Harrison. Brownian models of queueing networks with heterogeneous customer populations. In W. Fleming and P. L. Lions, editors, *Stochastic Differential Systems, Stochastic Control Theory and Applications*, volume 10 of *The IMA Volumes in Mathematics and Its Applications*, pages 147–186. Springer, New York, NY, 1988. doi:10.1007/978-1-4613-8762-6_11.
- [30] J. Michael Harrison. The bigstep approach to flow management in stochastic processing networks. In S. Zachary F. P. Kelly and I. Ziedins, editors, *Stochastic Networks: Theory and Applications*, volume 4 of *Lecture Note Series*, pages 57–90. Oxford University Press, 1996.
- [31] J Michael Harrison. Heavy traffic analysis of a system with parallel servers: asymptotic optimality of discrete-review policies. *The Annals of Applied Probability*, 8(3):822–848, 1998.
- [32] J. Michael Harrison. Brownian models of open processing networks: canonical representation of workload. *Ann. Appl. Probab.*, 10(1):75–103, 2000. corrections: **13**, 390–393 (2003) and **16**, 1703–1732 (2006). doi:10.1214/aoap/1019737665.
- [33] J. Michael Harrison. Stochastic networks and activity analysis. In Yu. M. Suhov, editor, *Analytic Methods in Applied Probability: In memory of Fridrikh Karpelevich*, volume 207 of *American Mathematical Society Translations: Series 2*, pages 53–76, Providence, RI, 2002. American Mathematical Society. doi:10.1090/trans2/207/04.
- [34] J. Michael Harrison and Viêt Nguyen. Brownian models of multiclass queueing networks: current status and open problems. *Queueing Systems. Theory and Applications*, 13(1-3):5–40, 1993.
- [35] J. Michael Harrison and Lawrence M. Wein. Scheduling networks of queues: heavy traffic analysis of a two-station closed network. *Operations Research*, 38(6):1052–1064, 1990.
- [36] Shane G. Henderson and Peter W. Glynn. Approximating martingales for variance reduction in Markov process simulation. *Mathematics of Operations Research*, 27(2):253–271, 2002.
- [37] Shane G. Henderson and Sean P. Meyn. Efficient simulation of multiclass queueing networks. In *Proceedings of the 29th conference on Winter simulation - WSC '97*, pages 216–223, New York, New York, USA, 1997. ACM Press.
- [38] Shane G. Henderson, Sean P. Meyn, and Vladislav B. Tadić. Performance evaluation and policy selection in multiclass networks. *Discrete Event Dynamic Systems: Theory and Applications*, 13(1-2):149–189, 2003.
- [39] Matteo Hessel, Joseph Modayil, Hado van Hasselt, Tom Schaul, Georg Ostrovski, Will Dabney, Dan Horgan, Bilal Piot, Mohammad Azar, and David Silver. Rainbow: Combining improvements in deep reinforcement learning. In *32nd AAAI Conference on Artificial Intelligence, AAAI*, pages 3215–3222, 2018.
- [40] A. Ilyas, L. Engstrom, S. Santurkar, D. Tsipras, F. Janoos, L. Rudolph, and A. M. Adry. A closer look at deep policy gradients. In *ICLR*, 2020. URL: <https://arxiv.org/abs/1811.02553>.

- [41] Tommi Jaakkola, Satinder P. Singh, and Michael I. Jordan. Reinforcement learning algorithm for partially observable Markov decision problems. In *Proceedings of the 7th International Conference on Neural Information Processing Systems*, pages 345–352, 1994.
- [42] Shuxia Jiang, Yuanyuan Liu, and Yingchun Tang. A unified perturbation analysis framework for countable Markov chains. *Linear Algebra and Its Applications*, 529:413–440, 2017.
- [43] Sham Kakade. Optimizing average reward using discounted rewards. In *COLT '01/EuroCOLT '01*, pages 605–615, 2001.
- [44] Sham Kakade and John Langford. Approximately optimal approximate reinforcement learning. In *Proceedings of the 19th ICML*, pages 267–274, 2002.
- [45] John G. Kemeny, J. Laurie. Snell, and Anthony W. Knapp. *Denumerable Markov Chains*. Springer New York, 1976.
- [46] Diederik P. Kingma and Jimmy Ba. Adam: A method for stochastic optimization. In *ICLR*, 2015. URL: <http://arxiv.org/abs/1412.6980>.
- [47] Vijay R. Konda and John N. Tsitsiklis. On actor-critic algorithms. *SIAM Journal on Control and Optimization*, 42(4):1143–1166, 2003.
- [48] P. R. Kumar. Re-entrant lines. *Queueing Systems. Theory and Applications*, 13(1-3):87–110, 1993.
- [49] Sunil Kumar and P. R. Kumar. Performance bounds for queueing networks and scheduling policies. *IEEE Transactions on Automatic Control*, AC-39:1600–1611, 1994.
- [50] Sunil Kumar and P. R. Kumar. Fluctuation smoothing policies are stable for stochastic reentrant lines. *Discrete Event Dynamic Systems*, 6:361–370, 1996.
- [51] Lucas Lehnert, Romain Laroche, and Harm van Seijen. On value function representation of long horizon problems. *Thirty-Second AAAI Conference on Artificial Intelligence*, 2018.
- [52] S. C. H. Lu, D. Ramaswamy, and P. R. Kumar. Efficient scheduling policies to reduce mean and variance of cycle-time in semiconductor manufacturing plants. *IEEE Transactions on Semiconductor Manufacturing*, 7(3):374–388, 1994.
- [53] Nguyen Cong Luong, Dinh Thai Hoang, Shimin Gong, Dusit Niyato, Ping Wang, Ying Chang Liang, and Dong In Kim. Applications of deep reinforcement learning in communications and networking: A survey. *IEEE Communications Surveys and Tutorials*, 21(4):3133–3174, 2019.
- [54] Constantinos Maglaras. Discrete-review policies for scheduling stochastic networks: trajectory tracking and fluid-scale asymptotic optimality. *The Annals of Applied Probability*, 10(3):897–929, aug 2000.
- [55] S.T. Maguluri, R. Srikant, and Lei Ying. Stochastic models of load balancing and scheduling in cloud computing clusters. In *INFOCOM, 2012 Proceedings IEEE*, pages 702–710, 2012.
- [56] Peter Marbach and John N. Tsitsiklis. Simulation-based optimization of Markov reward processes. *IEEE Transactions on Automatic Control*, 46(2):191–209, 2001.
- [57] L. F. Martins, S. E. Shreve, and H. M. Soner. Heavy traffic convergence of a controlled, multiclass queueing system. *SIAM Journal on Control and Optimization*, 34(6):2133–2171, 1996.
- [58] N. McKeown, A. Mekkittikul, V. Anantharam, and J. Walrand. Achieving 100% throughput in an input-queued switch. *IEEE Transactions on Communications*, 47(8):1260–1267, 1999.
- [59] Sean Meyn. Stability and optimization of queueing networks and their fluid models. In *Mathematics of Stochastic Manufacturing Systems (Williamsburg, VA, 1996)*, volume 33 of *Lectures in Applied Mathematics*, pages 175–199. American Mathematical Society, Providence, RI, 1997.
- [60] Sean Meyn. *Control Techniques for Complex Networks*. Cambridge University Press, Cambridge, 2007.

- [61] Sean Meyn and Richard L. Tweedie. *Markov Chains and Stochastic Stability*. Cambridge University Press, Cambridge, 2nd edition, 2009.
- [62] V. Mnih, K. Kavukcuoglu, D. Silver, A. A. Rusu, J. Veness, M. G. Bellemare, A. Graves, M. Riedmiller, A. K. Fidjeland, G. Ostrovski, S. Petersen, C. Beattie, A. Sadik, I. Antonoglou, H. King, D. Kumaran, D. Wierstra, S. Legg, and D. Hassabis. Human-level control through deep reinforcement learning. *Nature*, 518(7540):529–533, 2015.
- [63] Ciamac Moallemi, Sunil Kumar, and Benjamin Van Roy. Approximate and data-driven dynamic programming for queueing networks. Preprint, 2008.
- [64] P. Moritz, R. Nishihara, S. Wang, A. Tumanov, R. Liaw, E. Liang, M. Elibol, Z. Yang, W. Paul, M. I. Jordan, and I. Stoica. Ray: A distributed framework for emerging AI applications. 2018. URL: <http://arxiv.org/abs/1712.05889>.
- [65] Barry L. Nelson. Batch size effects on the efficiency of control variates in simulation. *European Journal of Operational Research*, 43(2):184–196, 1989.
- [66] OpenAI. Dota 2 with large scale deep reinforcement learning. 2019. URL: <http://arxiv.org/abs/1912.06680>.
- [67] I.C. Paschalidis, C. Su, and M.C. Caramanis. Target-pursuing scheduling and routing policies for multiclass queueing networks. *IEEE Transactions on Automatic Control*, 49(10):1709–1722, 2004.
- [68] J. R. Perkins and P. R. Kumar. Stable distributed real-time scheduling of flexible manufacturing/assembly/disassembly systems. *IEEE Transactions on Automatic Control*, AC-34:139–148, 1989.
- [69] Jan Peters and Stefan Schaal. Reinforcement learning of motor skills with policy gradients. *Neural Networks*, 21(4):682–697, 2008.
- [70] Martin L. Puterman. *Markov Decision Processes: discrete stochastic dynamic programming*. Wiley-Interscience, Hoboken, New Jersey, 2005.
- [71] Jose A. Ramirez-Hernandez and Emmanuel Fernandez. An approximate dynamic programming approach for job releasing and sequencing in a reentrant manufacturing line. In *2007 IEEE International Symposium on Approximate Dynamic Programming and Reinforcement Learning*, pages 201–208. IEEE, 2007.
- [72] John Schulman, Oleg Klimov, Filip Wolski, Prafulla Dhariwal, and Alec Radford. Proximal policy optimization. *OpenAI Blog*, 2017. URL: <https://openai.com/blog/openai-baselines-ppo/>.
- [73] John Schulman, Sergey Levine, Philipp Moritz, Michael I. Jordan, and Pieter Abbeel. Trust region policy optimization. In *Proceeding ICML’15*, pages 1889–1897, 2015. URL: <http://arxiv.org/abs/1502.05477>.
- [74] John Schulman, Philipp Moritz, Sergey Levine, Michael I. Jordan, and Pieter Abbeel. High-dimensional continuous control using generalized advantage estimation. In *ICLR*, 2016. URL: <https://arxiv.org/abs/1506.02438>.
- [75] John Schulman, Filip Wolski, Prafulla Dhariwal, Alec Radford, and Oleg Klimov. Proximal policy optimization algorithms. 2017. URL: <http://arxiv.org/abs/1707.06347>.
- [76] Richard F. Serfozo. Technical note - An equivalence between continuous and discrete time Markov decision processes. *Operations Research*, 27(3):616–620, 1979.
- [77] D. Silver, J. Schrittwieser, K. Simonyan, I. Antonoglou, A. Huang, A. Guez, T. Hubert, L. Baker, M. Lai, A. Bolton, Y. Chen, T. Lillicrap, F. Hui, L. Sifre, G. van den Driessche, T. Graepel, and D. Hassabis. Mastering the game of Go without human knowledge. *Nature*, 550(7676):354–359, 2017.

- [78] Gregor Simm, Robert Pinsler, and Jose Miguel Hernandez-Lobato. Reinforcement learning for molecular design guided by quantum mechanics. In *Proceedings of the 37th International Conference on Machine Learning*, volume 119, pages 8959–8969, 2020.
- [79] R. Srikant and Lei Ying. *Communication Networks: An Optimization, Control and Stochastic Networks Perspective*. Cambridge University Press, Cambridge, UK, 2014.
- [80] Richard S. Sutton and Andrew G. Barto. *Reinforcement learning: an introduction*. MIT press, 2nd edition, 2018.
- [81] Philip S Thomas. Bias in natural actor-critic algorithms. In *Proceedings of the 31st ICML*, 2014.
- [82] Michael H. Veatch. Approximate linear programming for networks: Average cost bounds. *Computers & Operations Research*, 63:32–45, 2015.
- [83] O. Vinyals, I. Babuschkin, . Czarnecki, W, and et.al. Grandmaster level in starcraft ii using multi-agent reinforcement learning. *Nature*, 575(7782):350–354, 2019.
- [84] Harvey M. Wagner. *Principles of Operations Research: with applications to managerial decisions*. Englewood Cliffs, N.J. : Prentice-Hall, 2nd edition, 1975.
- [85] Yuhui Wang, Hao He, Xiaoyang Tan, and Yaozhong Gan. Trust region-guided proximal policy optimization. In *Advances in Neural Information Processing Systems*, volume 32, pages 626–636, 2019.
- [86] Ziyu Wang, Victor Bapst, Nicolas Heess, Volodymyr Mnih, Remi Munos, Koray Kavukcuoglu, and Nando de Freitas. Sample efficient actor-critic with experience replay. In *ICLR*, 2017. URL: <http://arxiv.org/abs/1611.01224>.
- [87] R. J. Williams. Some recent developments for queueing networks. In *Probability Towards 2000*, pages 340–456. Springer, 1998.
- [88] Yuhuai Wu, Elman Mansimov, Shun Liao, Roger Grosse, and Jimmy Ba. Scalable trust-region method for deep reinforcement learning using Kronecker-factored approximation. In *Proceedings of the 31st International Conference on Neural Information Processing Systems*, pages 5285–5294, 2017.
- [89] Barret Zoph, Vijay Vasudevan, Jonathon Shlens, and Quoc V. Le. Learning transferable architectures for scalable image recognition. In *Proceedings of the IEEE Conference on Computer Vision and Pattern Recognition (CVPR)*, June 2018.